CIAMTIS

U.S. DOT Region 3 University Transportation Center

September 04, 2024

Prepared by:
**Hanbin Cheng, Aleksandra Radlińska -The Pennsylvania State University
Izhar Ahmad, Mehdi Shokouhian- Morgan State University**

r3utc.psu.edu

PennState
College of Engineering

LARSON
TRANSPORTATION
INSTITUTE

CIAMTIS
U.S. DOT Region 3 University Transportation Center

1

r3utc.psu.edu

DISCLAIMER

The contents of this report reflect the views of the authors, who are responsible for the facts and the accuracy of the information presented herein. This document is disseminated in the interest of information exchange. The report is funded, partially or entirely, by a grant from the U.S. Department of Transportation's University Transportation Centers Program. However, the U.S. Government assumes no liability for the contents or use thereof.

1. Report No. CIAM-UTC REG39	2. Government Accession No.	3. Recipient's Catalog No.	
4. Title and Subtitle Improving Freeze-thaw Resistance and Fatigue Resistance of Recycled Aggregate Concrete		**5. Report Date** Sep 04, 2024	
		6. Performing Organization Code	
7. Author(s) Hanbin Cheng Aleksandra Radlińska Izhar Ahmada Mehdi Shokouhiana		**8. Performing Organization Report No.**	
9. Performing Organization Name and Address The Pennsylvania State University 201 Old Main, University Park, PA 16802 Morgan State University 1700 E Cold Spring Ln, Baltimore, MD 21251		**10. Work Unit No. (TRAIS)**	
		11. Contract or Grant No.[3900039095/PSUCIAMTIS2019	
12. Sponsoring Agency Name and Address U.S. Department of Transportation Research and Innovative Technology Administration 3rd Fl, East Bldg E33-461 1200 New Jersey Ave, SE Washington, DC 20590		**13. Type of Report and Period Covered** Draft Final Report 12/31/2023 – 09/04/2024	
		14. Sponsoring Agency Code	

16. Abstract

The use of recycled aggregate concrete (RAC) in pavement infrastructure provides a sustainable solution to address construction waste. However, RAC typically suffers from poor freeze-thaw resistance and reduced fatigue life due to the undesirable properties of recycled aggregates. This study explores three modification treatments—silane surface modification, sodium silicate surface modification, and silane internal modification—to improve RAC's durability and fatigue performance under freeze-thaw conditions. The modified RAC was evaluated based on mass loss ratio, compressive strength, relative elastic modulus, water permeability, and flexural strength during freeze-thaw cycles. Using scanning electron microscopy (SEM) and backscattered electron imaging (BSE), the microstructure of the recycled aggregates and the ITZ between aggregates and the cement matrix were analyzed. Additionally, fatigue life was assessed after 0, 70, and 140 freeze-thaw cycles at stress levels of 0.6, 0.7, and 0.8, and a fatigue life model was developed. The results indicate that the proposed treatments significantly enhance the freeze-thaw durability and fatigue resilience of RAC. This study supports the broader use of recycled aggregates in sustainable pavement construction.

17. Key Words Recycled aggregate concrete, Freeze-thaw resistance, Fatigue life, Aggregate surface modification, Cement matrix modification		18. Distribution Statement No restrictions. This document is available from the National Technical Information Service, Springfield, VA 22161	
19. Security Classif. (of this report) Unclassified	**20. Security Classif. (of this page)** Unclassified	**21. No. of Pages** 67	**22. Price**

Form DOT F 1700.7　　　　　**(8-72)   Reproduction of completed page authorized**

CIAMTIS
U.S. DOT Region 3 University Transportation Center

r3utc.psu.edu

Table of Contents

CIAMTIS
U.S. DOT Region 3 University Transportation Center

Lists of Figures

Lists of Tables

U.S. DOT Region 3 University Transportation Center

CHAPTER 1

Introduction

BACKGROUND

The world has witnessed a dramatic increase in urbanization over recent decades. According to the United Nations Department of Economic and Social Affairs, more than 55% of the global population now resides in urban areas, and this figure is projected to rise to 68% by 2050 [1]. This rapid urban expansion has resulted in the generation of substantial amounts of construction and demolition (CD) waste, produced from activities such as new construction projects, renovations, demolitions, and roadwork. In the United States alone, approximately 30% of the total annual CD waste is generated, amounting to an estimated 534 million tons in 2014 [2]. Historically, CD waste has been viewed as a low-value material, commonly disposed of in landfills. However, improper disposal of CD waste not only leads to significant environmental concerns such as land and groundwater pollution, but it also consumes valuable land resources [3,4].

To mitigate the environmental impact of CD waste, extensive research has focused on sustainable solutions, particularly through the reuse of recycled aggregates (RA) in construction [5-10]. The performance of concrete made with recycled aggregates has been rigorously studied. However, research indicates that increasing the RA replacement ratio often results in diminished mechanical properties and reduced freeze-thaw resistance, limiting the broader use of recycled aggregates. These challenges are primarily due to the undesirable properties of RA, such as the presence of micro-cracks in the aged cement paste and the formation of a poor interfacial transition zone (ITZ) between the recycled aggregate and the new cement matrix.

Several traditional approaches have been employed to improve the freeze-thaw resistance of recycled aggregate concrete (RAC), including the addition of fly ash, silica fume, and fibers to the cement paste. However, these methods fail to address the fundamental weaknesses of RA itself [11-20]. Unlike natural aggregates, recycled aggregates tend to have a higher water absorption capacity due to the presence of aged cement paste. This requires the addition of extra water to achieve sufficient workability. However, the excess water retained in the recycled aggregates is later released during the mixing and curing processes, leading to the formation of a weaker ITZ, which compromises both the mechanical strength and freeze-thaw durability of the concrete. Given these limitations, modifying the properties of RA becomes essential for enhancing the performance of RAC.

To improve the durability of RAC, a variety of RA treatment methods have been investigated [21-23]. Autogenous cleaning has been proposed as a method for removing the loosely adhered old mortar from the surfaces of recycled aggregates. Research has identified the picking method as particularly effective in this context. Although chemical treatments have shown promise in reducing water absorption, they raise environmental concerns due to the potential for residual acid ions in the aggregate to compromise the durability of the concrete. Pre-soaking RA in cementitious materials has also been explored, though this approach is labor-intensive. An alternative method involves pretreatment with sodium silicate solution,

which has been found to reduce both the water absorption and the crushing index of RA. Surface modification using silane emulsion has also demonstrated efficacy in reducing water absorption by forming a hydrophobic film on the surface of the recycled aggregate.

Despite these advancements, much of the current research on RA surface modification has largely overlooked its effects on the fatigue behavior of RAC—an important consideration for practical applications, particularly for structures subjected to cyclic loading such as pavements and highway bridges. The fatigue resistance of RAC remains underexplored in comparison to conventional concrete, and studies examining the effects of freeze-thaw cycles on the fatigue performance of RAC are even more limited. This is a significant gap in the research, as freeze-thaw damage is a critical factor influencing the long-term durability of concrete in cold climates [24-27].

This report addresses this research gap by focusing on the freeze-thaw resistance and fatigue behavior of recycled aggregate concrete (RAC) subjected to freeze-thaw damage. Four groups of RAC were prepared: one control group, two groups with surface-modified recycled aggregates treated with either sodium silicate solution or silane emulsion, and a fourth group incorporating a silane-modified cement matrix. Key performance indicators such as compressive strength, flexural strength, permeability, mass loss ratio, and dynamic elastic modulus were measured under freeze-thaw conditions to evaluate the durability and performance of the RAC samples.

A central aspect of this study is the investigation of the fatigue behavior of RAC exposed to freeze-thaw damage at various stress levels. To model and predict the fatigue life of RAC under these conditions, failure distribution models and fatigue life prediction models were developed. Additionally, the mechanisms behind the performance improvements of RAC with different modifications were explored through detailed analyses of the interfacial transition zone (ITZ) between the recycled aggregates and the new cement matrix. These analyses were conducted using backscattered electron (BSE) imaging and scanning electron microscopy (SEM), offering valuable insights into the microstructural changes that enhance RAC durability.

The findings from this research provide a solid theoretical foundation and offer practical recommendations for the broader use of recycled aggregates in infrastructure construction. By addressing the challenges related to freeze-thaw resistance and fatigue behavior, this study contributes to the advancement of sustainable construction practices, paving the way for greater adoption of recycled materials in the built environment.

OBJECTIVES

To enhance the wide application of recycled aggregates in the transoporation infrastructure, we proposed several modification methods to enhance recycled aggregates and recycled aggregate-based concrete. Mechanical performance, durability and fatigure behavior of recycled aggregate-based concrete was investigated, and the optmial modification was identified.

Materials, methodology and evaluation

INTRODUCTION

This part summarize the methodology and evaluations used in the report.

Materials

In this study, Type I cement, conforming to ASTM C-150 and AASHTO M-85 standards, was utilized. The cement was supplied by the Lehigh Cement Company, with its chemical composition and specific gravity provided in Table 1. The cement met all required specifications for use in concrete mixtures for infrastructure applications. River sand, with a maximum particle size of 4.75 mm, was employed as the fine aggregate. The sand was selected for its consistent grading and cleanliness, making it suitable for concrete mixing.

For the recycled coarse aggregate, crushed concrete debris from demolished structures was used, with particle sizes ranging from 4.75 mm to 19 mm. The recycled aggregates had an LA abrasion loss [30,31] of 37.28%, indicating a moderate resistance to degradation under mechanical wear, which is a common property of recycled materials. The water absorption rate and oven-dried density of the recycled aggregates were measured according to ASTM C127 [28], yielding values of 7.53% and 2227 kg/m³, respectively, as shown in Table 2. The relatively high water absorption rate is characteristic of recycled aggregates, primarily due to the adhered mortar on the surface, which affects the overall performance of the concrete.

The particle size distribution of both the cement and aggregates is illustrated in Figure 1 and 2 , providing insight into the gradation and compatibility of the materials used. Additionally, silane emulsion, with a 40% concentration of triethoxyoctylsilane, was procured from BASF for use in surface modification of the recycled aggregates and the cement matrix. This silane emulsion was chosen for its ability to impart hydrophobic properties to the recycled aggregates, thus enhancing the freeze-thaw resistance and long-term durability of the RAC. The molecular structure of triethoxyoctylsilane is also depicted in Figure 3, highlighting the active component responsible for the chemical modification.

To improve the workability of the concrete, a superplasticizer (MasterGlenium 7620) [29], also supplied by BASF, was incorporated into the mix. This admixture allowed for a reduction in the water-to-cement ratio while maintaining a high level of workability, a critical factor in achieving the desired mechanical properties of the concrete.

Sodium silicate, another surface modification agent, was employed for the treatment of the recycled aggregates. This compound consisted of 27% Na_2O, 54% SiO_2, and 19% water, with a SiO_2/Na_2O molar ratio (also known as the water-glass modulus) of 2.07. Sodium hydroxide (98% purity NaOH pellets) was utilized as a reagent to adjust the water-glass modulus as necessary, optimizing the chemical interactions

between the recycled aggregates and the cement matrix. The sodium silicate treatment was expected to enhance the integrity of the interfacial transition zone (ITZ) and reduce the water absorption capacity of the recycled aggregates, ultimately contributing to improved freeze-thaw resistance and fatigue life of the RAC.

This careful selection of materials and additives reflects the experimental focus on improving the mechanical performance and durability of recycled aggregate concrete, particularly under conditions of freeze-thaw cycling, which is critical for infrastructure applications in cold climates. The use of both silane and sodium silicate for surface modification provides a comparative evaluation of their efficacy in mitigating the adverse effects of recycled aggregates on concrete performance, with particular attention to the enhancement of the ITZ and the overall durability of the concrete.
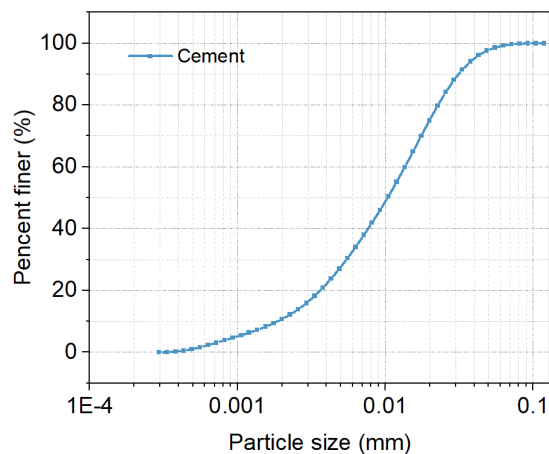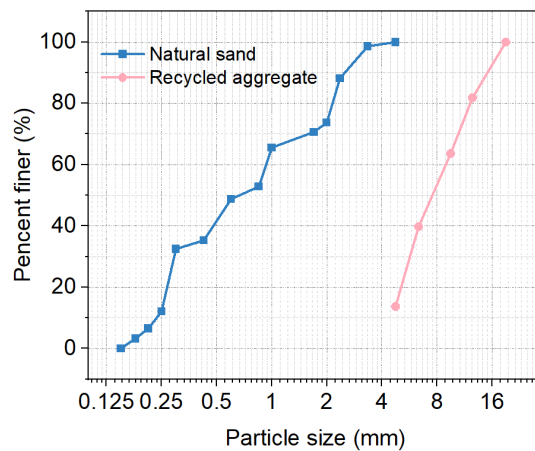

Fig.1 Particle size distribution of cement

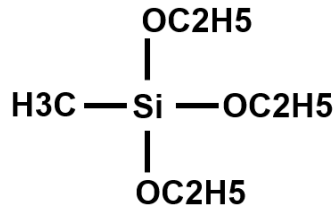**Fig.2 Particle size distribution of sand and recycled aggregate**

```
                OC2H5
                  |
H3C ── Si ── OC2H5
                  |
                OC2H5
```

Fig.3 Structural formula of MTES

Table.1 Cement composition

Item	Chemical content (%)								Specific gravity
	SiO$_2$	Al$_2$O$_3$	Fe$_2$O$_3$	CaO	MgO	Na$_2$O	SO$_3$	K$_2$O	
Cement	19	4.88	2.31	63.15	2.97	0.36	3.22	0.98	3.14

Table.2 Properties of the RA with and without surface modification

Property	Unmodified	Silane surface modified	Sodium silicate modified
Apparent density (kg/m3)	2677.77	2690.31	2695.43
Oven-dried density (kg/m3)	2227.89	2239.87	2250.65
Water absorption (%)	7.52	4.68	3.58
LA abrasion loss (%)	37.28	36.94	35.99

Modifications-silane emulison recycled aggregate surface modification

Compared to natural aggregates, recycled aggregates typically exhibit higher porosity, which poses significant challenges when they are introduced into concrete mixtures. One of the primary effects of this increased porosity is a reduction in the flowability of the concrete. To compensate for this, additional water is often added to wet the recycled aggregates during the mixing process. However, once the concrete is cast, the water stored within the recycled aggregates is gradually released, leading to increased porosity within both the interfacial transition zone (ITZ) and the surrounding cement matrix. This elevated porosity significantly compromises the freeze-thaw resistance of recycled aggregate concrete (RAC), making it less durable in environments subject to cyclical freezing and thawing.

To address these challenges and enhance the freeze-thaw resistance of RAC, surface modification treatments, such as silane modification and silica modification, have been employed. Among these, silane modification offers two distinct approaches: surface modification of the recycled aggregates and modification of the cement matrix using silane.

The process of silane surface modification for recycled aggregates is as follows:

Preparation of Silane Emulsion: The purchased silane emulsion is diluted to create a 5% solution.
Application: This diluted silane emulsion is sprayed onto the surface of the recycled aggregates.
Drying: The treated recycled aggregates are then left to dry at room temperature for 2 hours.
**Reapplication**: The spraying and drying steps are repeated for a total of eight rounds.

Final Drying: After the final application, the modified recycled aggregates are allowed to dry for four days in a controlled indoor environment.

Following this treatment, the water absorption of the modified recycled aggregates is significantly reduced to 4.68%. The reduction in water absorption is primarily due to the formation of a hydrophobic membrane on the surface of the recycled aggregates. This membrane acts as a barrier to moisture, thereby improving the overall durability of the aggregates when exposed to freeze-thaw conditions.

The underlying mechanism of this modification process is depicted in Figure 4. The surface of unmodified recycled aggregates is characterized by a porous and rough texture, which allows for high water absorption. In contrast, the modified recycled aggregates are coated with a silicone-based membrane that reduces this porosity. The formation of this membrane occurs through a series of chemical reactions. First, the ethoxy groups of methyltriethoxysilane (MTES) undergo hydrolysis in the alkaline environment provided by the recycled aggregates, converting to hydroxyl groups. These hydroxyl groups then participate in a condensation reaction, resulting in the formation of Si–O–Si bonds. As moisture evaporates from the solution, a hydrophobic silicone membrane forms, coating the surface of the recycled aggregates. This membrane is responsible for the reduced water absorption and improved freeze-thaw resistance of the modified recycled aggregates.

Silane modification thus proves to be an effective strategy in mitigating the inherent weaknesses of recycled aggregates, particularly in enhancing their durability under harsh environmental conditions. By reducing water absorption and improving the integrity of the ITZ, this treatment helps extend the service life of RAC in freeze-thaw environments. Moreover, the development of a stable hydrophobic coating through silane modification contributes to the long-term performance and sustainability of recycled aggregate concrete, making it a viable alternative for use in infrastructure projects.

Fig.4 Silane surface modification method
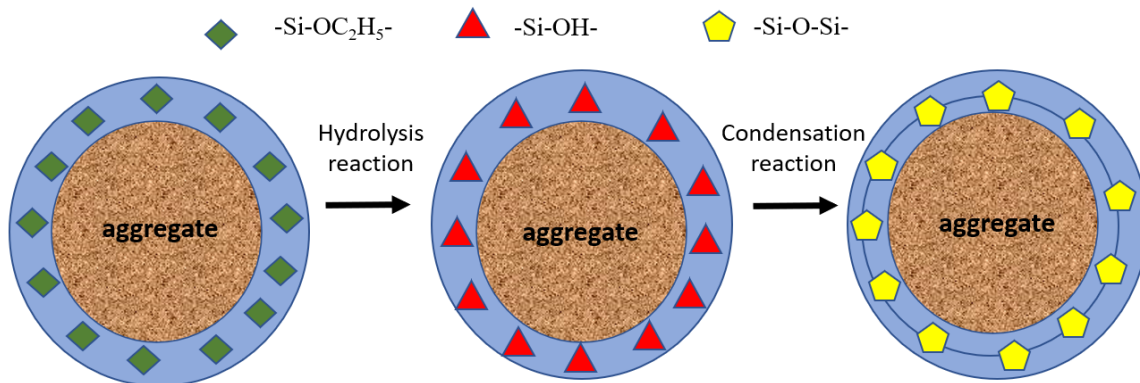
Modifications-silane emulsion cement matrix modification

The silane cement matrix modification method involves incorporating a specific dosage of silane emulsion directly into the mixing water used for concrete preparation. This modification technique aims to enhance the freeze-thaw resistance of recycled aggregate concrete (RAC) by forming a hydrophobic silicone membrane within the cement matrix. The hydrophobic nature of this silicone membrane significantly reduces water infiltration, thereby mitigating the damage caused by freeze-thaw cycles—a common issue in concrete durability. By preventing water from penetrating the matrix, this method helps to protect the recycled aggregate concrete from internal damage due to freezing and thawing.

CIAMTIS
U.S. DOT Region 3 University Transportation Center

However, the inclusion of silane emulsion in the cement matrix, while beneficial for water resistance, has been observed to negatively impact the compressive strength of the concrete. This reduction in strength is a critical consideration, as it may limit the structural performance of the concrete. Therefore, it is essential to determine an optimal dosage of silane emulsion that balances improved water resistance with minimal strength reduction.

To identify this optimal dosage, a series of cement paste samples were prepared with varying silane emulsion content. The selected dosages included 0%, 0.2%, 0.6%, and 0.8% of the cement weight. These specific dosage levels were chosen to assess the progressive effect of silane emulsion on both the mechanical and durability properties of the concrete. All samples maintained a constant water-to-binder ratio of 0.52 to ensure consistency across the tests. The compressive strength of the cement paste samples will be measured after 28 days of curing, providing insight into the effect of silane emulsion on the mechanical strength of the matrix.

In addition to measuring compressive strength, the water resistance of the silane-modified cement matrix will be evaluated according to ASTM C1585, the standard test method for determining the rate of water absorption in cementitious materials. This test will assess the ability of the modified cement matrix to resist water ingress, a key factor in preventing freeze-thaw damage. By comparing the results of water absorption and compressive strength across different silane dosages, the study aims to determine the dosage that provides the most effective balance between enhancing freeze-thaw resistance and maintaining structural integrity.

The formation of the hydrophobic silicone membrane within the cement matrix is the primary mechanism through which silane modification enhances water resistance. The silicone membrane reduces capillary water absorption, thus limiting the movement of moisture through the concrete. This is particularly important in environments where concrete is subjected to cyclical freezing and thawing, as the presence of water within the matrix can lead to internal cracking and spalling. By reducing water absorption, the silane-modified matrix helps to preserve the concrete's integrity under these harsh conditions.

However, the potential reduction in compressive strength caused by the inclusion of silane emulsion remains a challenge. Previous studies have shown that the addition of silane can interfere with the hydration process of cement, leading to weaker bonds within the matrix. Therefore, this study seeks to optimize the dosage of silane emulsion to achieve the desired freeze-thaw resistance without excessively compromising the mechanical properties of the concrete.

Through the combined analysis of compressive strength and water resistance, this research will provide valuable insights into the effectiveness of silane cement matrix modification. The results will offer a foundation for optimizing the use of silane emulsion in recycled aggregate concrete, ultimately contributing to the development of more durable and sustainable concrete materials for infrastructure applications.

The freeze-thaw resistance of recycled aggregate concrete (RAC) can be significantly enhanced through cement matrix modification using silane emulsion. A 5% diluted silane emulsion is typically mixed with the cement to perform this modification. However, while this treatment improves the water resistance and durability of the concrete, it also reduces the hydration degree of the modified cement paste, leading to a potential reduction in strength. Therefore, determining an optimal dosage of silane emulsion is crucial to strike a balance between strength preservation and durability enhancement.

In this study, cement paste was blended with varying dosages of silane emulsion: 0%, 0.2%, 0.4%, and 0.6% by weight of cement. A consistent water-to-binder ratio of 0.52 was maintained for all mixtures to ensure uniformity. To evaluate the effects of silane on the mechanical and durability properties of the modified cement paste, 2-inch cubes were prepared for compressive strength testing after 28 days of standard curing, following ASTM C109 guidelines. Additionally, disc samples were cast to measure water absorption rates, adhering to ASTM C1585 standards. These tests aimed to assess both the compressive strength and the water diffusion resistance of the modified cement paste.

The results, as shown in Figure 5, indicate that increasing the proportion of silane emulsion in the cement paste correlates with a reduction in compressive strength. This reduction in strength is primarily attributed to the impediment of cement hydration caused by the presence of silane. The silane emulsion, while forming a hydrophobic layer within the cement matrix, can also interfere with the normal hydration process, resulting in incomplete bond formation between the cement particles. As a result, higher silane concentrations tend to weaken the overall matrix structure.

Despite this reduction in strength, the inclusion of silane emulsion provides a marked improvement in water resistance. The silane forms a silicone-based hydrophobic membrane within the cement matrix, which effectively reduces water permeability. This reduction in water diffusion is particularly advantageous for improving freeze-thaw resistance, as it minimizes the amount of moisture that can penetrate the concrete, thereby preventing internal freezing and subsequent damage. The results reveal that an increasing dosage of silane emulsion reduces water permeability, with the most significant improvements observed at lower dosages.

However, it is important to note that the improvement in water diffusion resistance becomes limited when the silane dosage exceeds 0.4% by weight of cement. At dosages beyond this point, the hydrophobic membrane reaches its maximum effectiveness, and further increases in silane content do not yield additional benefits in water resistance. On the contrary, higher dosages continue to impede the hydration process, leading to further reductions in strength without corresponding gains in durability.

Based on these findings, the optimal dosage of silane emulsion for cement matrix modification is determined to be 0.4% by weight of cement. At this dosage, the silane emulsion offers a balanced trade-off between compressive strength preservation and water diffusion resistance. The 0.4% dosage achieves significant improvement in water resistance while minimizing the negative impact on strength, making it the most effective formulation for enhancing the freeze-thaw durability of RAC without excessively compromising its mechanical performance.
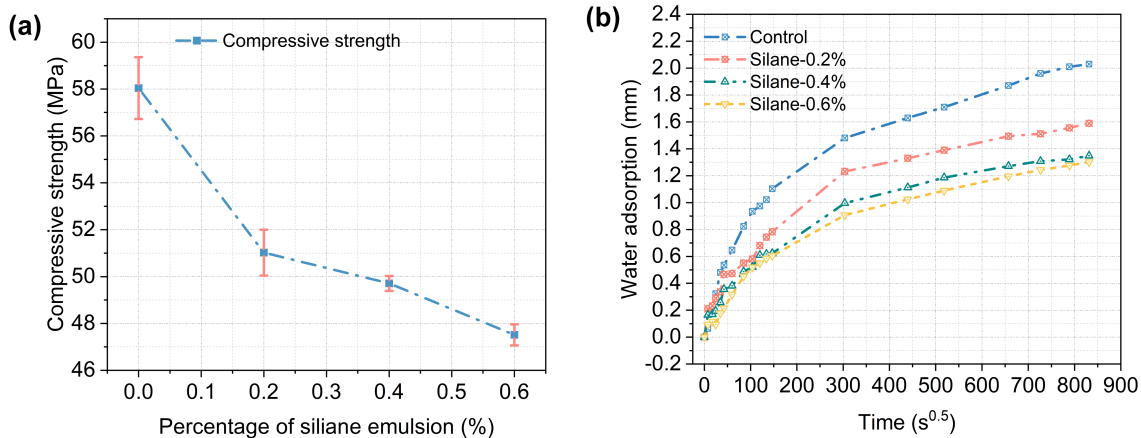
.

Fig.5 Influence of silane emulision of perfromacne of cement paste; (a) compressive strength of samples; (b) water absorption rate of samples.

Modifications-sodium silicate recycled aggregate surface modification

In this study, sodium silicate was employed to perform surface modification on recycled aggregates (RA) to improve their properties, particularly by reducing porosity and water absorption. The detailed process for this surface modification technique is outlined as follows:

Preparation of Sodium Silicate Solution: A 5% sodium silicate solution was prepared using water heated to a temperature of 45°C. The elevated temperature is critical for ensuring that the solution remains in a highly reactive state, promoting effective surface treatment.

Immersion of Recycled Aggregates: The recycled aggregates were immersed in the prepared sodium silicate solution at 45°C for 1.5 hours. This duration allows sufficient time for the chemical interactions between the sodium silicate and the surface of the recycled aggregates to take place, enabling the treatment to penetrate effectively into the aggregate structure.

Drying Process: After the immersion treatment, the aggregates were removed from the solution and dried in an oven set to 45°C for four days. This drying phase is essential for ensuring the stabilization of the chemical products formed on the surface of the aggregates.

As a result of this treatment, the water absorption of the modified recycled aggregates was significantly reduced, decreasing from 7.5% to 3.58%. This reduction is attributed to the chemical reaction between sodium silicate and the hydroxyl groups present on the surface of the recycled aggregates, leading to the formation of calcium silicate hydrate (C-S-H) gel. C-S-H is a key component in the hydration process of cementitious materials and is known for its ability to fill voids and micro-cracks within materials. In this case, the C-S-H gel fills the pores and voids on the surface of the recycled aggregates, effectively reducing their porosity.

The reduction in porosity is a crucial improvement, as the high porosity of untreated recycled aggregates is one of the primary factors contributing to their poor performance in concrete applications. Porous

aggregates tend to absorb more water during the concrete mixing process, which can lead to excessive internal voids and a weakened interfacial transition zone (ITZ) between the aggregate and the cement matrix. By lowering the water absorption capacity of the recycled aggregates through sodium silicate treatment, these issues are mitigated, resulting in a more robust and durable recycled aggregate concrete (RAC).

The formation of the C-S-H gel on the aggregate surface enhances the bonding between the recycled aggregates and the surrounding cement paste, creating a denser and stronger ITZ. This improvement in the ITZ is particularly significant for enhancing the mechanical performance of RAC, as a stronger bond at the interface contributes to higher compressive strength and improved durability, particularly under conditions of freeze-thaw cycling or other environmental stressors.

In summary, the sodium silicate surface modification technique offers a highly effective approach to improving the quality of recycled aggregates by reducing their porosity and water absorption. Through the formation of C-S-H gel, the treatment enhances the aggregate-cement bond, leading to improved mechanical properties and long-term durability of the concrete. This modification technique contributes to advancing the sustainability of recycled aggregates in concrete applications, making them more viable for use in infrastructure projects that demand high-performance materials.

Mix proportion and sample preparation

In this study, four groups of recycled aggregate (RA) permeable concrete were designed: ''Control'' (C), ''Silane Surface Modification'' (S-M), ''Silane Integral Modification'' (SI-M), and ''Sodium Silicate Surface Modification'' (SS-M). The mix proportions for each group are detailed in Table 3. The primary distinction among the groups lies in the modification treatments applied to the recycled aggregates or the cement matrix.

In the SSM group, the surface of the recycled aggregates was modified using a silane emulsion. This surface treatment is intended to reduce water absorption and enhance the freeze-thaw resistance of the RA concrete. Conversely, in the SIM group, the silane emulsion was introduced directly into the cement paste, modifying the matrix itself rather than the aggregate surface. This integral modification aims to form a hydrophobic barrier throughout the cement matrix to improve water resistance and durability. In the SSSM group, sodium silicate was used to treat the surface of the recycled aggregates, forming a calcium silicate hydrate (C-S-H) gel that fills voids and reduces aggregate porosity, thereby improving the performance of the concrete.

To ensure proper mixing and consistency across all groups, additional water was used to bring the recycled aggregates to a surface-saturated condition before mixing. The mixing process for all groups followed the same standardized procedure, which is described as follows:

Initial Mixing: Sands and recycled aggregates were mixed with half of the total mixing water for 120 seconds to ensure thorough wetting and cohesion of the materials.
Addition of Cement: Cement was then added to the mixer and blended with the aggregates for 20 seconds to begin the formation of the paste.
Final Mixing: The remaining mixing water, along with a superplasticizer, was introduced, and the mixture was blended for an additional 130 seconds to achieve the desired workability and consistency.
To assess the performance of the modified concrete, various specimens were prepared for mechanical and durability testing. Three prismatic specimens, each measuring 75 mm × 75 mm × 400 mm, were cast for

CIAMTIS
U.S. DOT Region 3 University Transportation Center

each group to conduct freeze-thaw resistance tests. These specimens were subjected to cyclic freeze-thaw conditions to evaluate the durability and resilience of the modified concrete in environments prone to temperature fluctuations.

In addition, 56 cylindrical specimens, each measuring 76.2 mm × 152.4 mm, were prepared for each group to assess the compressive strength of the concrete. The compressive strength tests were performed following the standard testing procedures to determine the mechanical performance of the concrete under load. All specimens were molded with extra compaction to ensure uniformity and to minimize voids within the concrete matrix. After molding, the specimens were cured in water for 28 days at a constant room temperature of 23°C to allow for full hydration and strength development.

The combination of freeze-thaw testing and compressive strength evaluation provided comprehensive insight into the mechanical and durability characteristics of the RA permeable concrete modified by silane and sodium silicate. This study contributes valuable information on the effectiveness of different surface and integral modification strategies in improving the long-term performance of recycled aggregate concrete, particularly under challenging environmental conditions.

Table.3 Mixing proportions of recycled aggregates concrete

ID	Cement	Water	Sand	RCA	Add-water	SP
C					7.5%	
S-M	405	210	680	1110	4.5%	0.7%
SS-M					7.5%	
SI-M					3.5%	

Evaluations

Freeze-thaw test and macroscopic investigations

The compressive strength of RAC was measured according to ASTM C-39 [32]. The flexural strength of specimens was determined according to ASTM C78 [33]. The water permeability of concrete was assessed using ASTM C1585 [34] on samples with 100 mm diameter and 50 mm height. The side surface of the samples was covered with a water- and vapor-tight film to ensure unidirectional water diffusion. Firstly, the dry mass of the samples was measured. The weight of samples was measured after the immersion to a depth of 5 mm water for 1, 5, 10, 20, 30 min, 1, 2, 3, 4, 5, 6 h, and once a day up to 8 days. The water absorption of samples can be calculated according to Eq. (2):

$$I = \frac{m_t}{a \times d} \tag{2}$$

Where, I the water absorption of samples, m_t is the change in specimen mass in grams, at the time t, a refers to the exposed area of the specimen, in mm^2, and d is the density of the water in g/mm3
The freeze-thaw durability test was carried out following ASTM C666 [35]. Mass (W_t) and longitudinal natural frequency (f_t) were measured every 35 cycles. The mass loss ratio can be calculated by Eq. (3):

$$\Delta W_t = \frac{W_0 - W_t}{W_0} \times 100\% \tag{3}$$

Where, ΔW_t is the mass loss ratio after t cycles, and W_t refers the mass after t cycles; W_0 stands for the initial mass.

The relative dynamic elastic modulus (RDEM) after t cycles of freeze-thaw damage can be determined according to Eq. (4):

$$RDEM_t = \frac{f_t^2}{f_0^2} \times 100\% \qquad (4)$$

Where $RDEM_t$ indicates the value of RDEM after t cycles, f_0 refers to the initial natural frequency, and f_t stands for the natural frequency after t cycles of freeze-thaw.

The longitudinal nature frequency was measured according to ASTM C215 [36]. The test system was composed of an impact hammer, and data acquisition system, and an acceleration sensor (see Fig. 6).
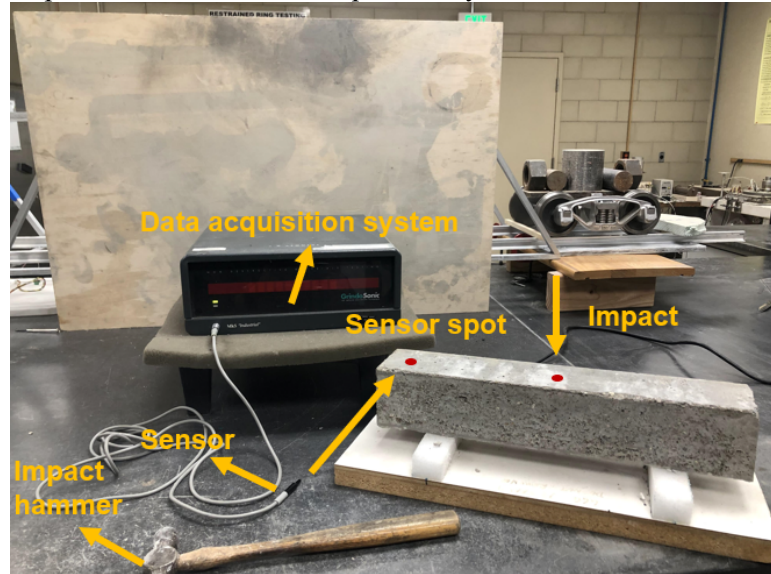

Fig.6. The test system for analyzing natural frequency

Microscale investigations

Backscattered electron image analysis (BSE-IA) was employed to perform a quantitative analysis of the microstructure of recycled aggregate concrete (RAC). This technique combines backscattered electron (BSE) imaging with advanced image analysis processing to differentiate and quantify various phases within cement-based materials. Typically, cement-based materials consist of pores, hydration products, and unhydrated cement, each of which displays a characteristic range of gray values in a BSE image. These gray values provide a means of distinguishing the different phases within the material, allowing for detailed microstructural analysis.

To accurately determine the gray value ranges corresponding to different material phases, the image intensity method was utilized. This method involves analyzing the second derivative of the cumulative distribution curve of the gray values within the image. The second derivative curve helps identify distinct inflection points, which serve as thresholds separating the different phases.

In Figure 7(a), a typical backscattered electron image of RAC is presented. The corresponding cumulative distribution of gray values is depicted in Figure 7(b). Based on the second derivative curve of this distribution, specific thresholds for different phases were established. For instance, pores were identified with gray values in the range of 0–120, while anhydrous (unhydrated) cement was characterized by gray

values between 177 and 255. These thresholds provide a clear demarcation between the material's phases, allowing for precise quantification.

To validate the determination of these gray value thresholds, a detailed analysis was performed. First, a localized area within Figure 7(a) was selected for further scrutiny, marked by a blue blank. This region included representative portions of pores, the hydrated cement matrix, and anhydrous cement. An assistant line was drawn from the origin (O) across the pore and the anhydrous cement region, as depicted in Figure 7(d). The gray value distribution along this line was extracted and is shown in Figure 7(e).

By comparing the gray value distribution along this line with the proposed thresholds for pores and anhydrous cement, it was confirmed that the assigned gray value ranges were accurate. The clear correspondence between the observed gray values and the material phases demonstrates the reliability of the threshold selection process. This method of using the second derivative of the cumulative gray value distribution allows for an objective and reproducible approach to phase identification within cement-based materials.

In summary, the BSE-IA technique, combined with image intensity analysis, provided a robust means of quantitatively assessing the microstructure of RAC. The validation of gray value thresholds enhances the accuracy of phase identification, contributing to a more detailed understanding of the microstructural characteristics that influence the mechanical and durability properties of RAC. This method offers significant potential for further research in the field of cementitious materials, particularly in relation to the performance of recycled aggregates in concrete.
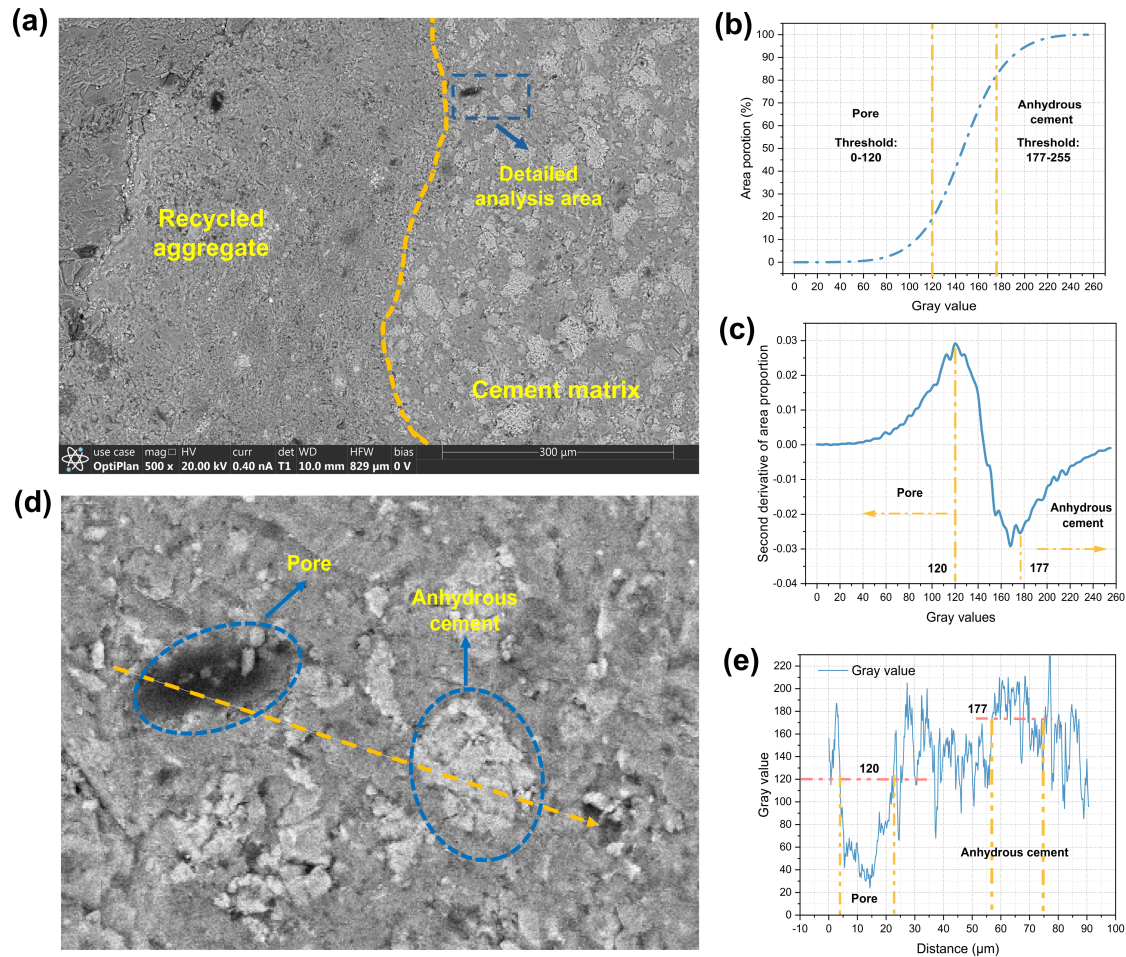
Fig.7 BSE image analysis; (a) typical case of RAC; (b) cumulative distribution of gray value; (c) secondary derivative cure of cumulative distribution curve of gray value; (d) a detailed local area; (e) the distribution of gray value along the assistant line

Flexural fatigue tests

The four-point bending fatigue test was performed on all specimens using an MTS fatigue machine after subjecting them to freeze-thaw cycles of 0, 70, and 140. This test aimed to assess the fatigue performance of recycled aggregate concrete (RAC) under different freeze-thaw conditions, providing insight into the durability of the modified concrete under cyclic loading. Three stress levels—0.6, 0.7, and 0.8—were selected for the fatigue tests on all samples. These levels were chosen to represent varying degrees of stress intensity, allowing for a comprehensive analysis of the fatigue behavior under different loading conditions. The stress ratio (defined as $f$min/$f$max) was set to 0.1, where $f$min and $f$max correspond to the minimum and maximum loads in each cycle of the sinusoidal wave. This stress ratio ensures that the specimens experience cyclic loading with significant variations in load, simulating realistic conditions that concrete would encounter in practical applications such as pavements or bridge decks.

A schematic representation of the four-point bending test setup is shown in Figure 8. In this configuration, the load is applied at two points along the span of the specimen, ensuring that the

maximum bending moment occurs between the loading points. This setup is advantageous as it creates a uniform moment region, allowing for a more accurate evaluation of the flexural fatigue performance of the concrete. By using this method, the fatigue life of the specimens under different freeze-thaw cycles and stress levels can be compared, providing valuable data on how freeze-thaw damage affects the longevity and mechanical properties of RAC.

The results of this test will contribute to the development of fatigue life prediction models for RAC under freeze-thaw conditions. These models will help in predicting the performance of RAC in real-world infrastructure subjected to cyclic loading and environmental stressors, offering guidance on the optimal use of recycled aggregates in concrete for durable, long-lasting structures.
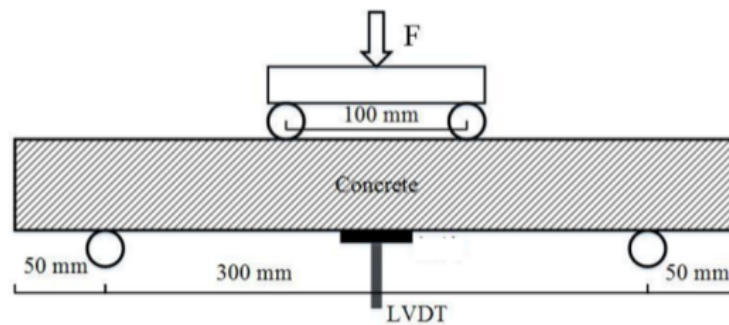
Fig.8. The test system for the flexural fatigue test

Numerical Modelling

The numerical analysis aimed to develop an RAC pavement slab section and analyze it for the maximum load-carrying capacity. For this purpose, ATENA studio version 5.9.2c was adopted as a non-linear analysis tool developed by Cervenka Consulting. This software can simulate the actual behavior of degradation in concrete material, yielding steel rebars in concrete structures and concrete crushing. CC3DNonLinCementitious2 model was used to combine fracture-plastic constitutive relations accounting for the non-linear behavior of concrete in the current study [37]. The detailed explaination is shown in the chapter 6.

CHAPTER 3

Findings on freeze-thaw damages of recycled aggregate concrete

Water permeability

Figure 9 presents the water absorption rate of recycled aggregate concrete (RAC) as a function of the square root of time. The results show that the water absorption of the samples does not follow the typical t-law (proportional to the square root of time), which is consistent with findings from previous studies. This deviation is attributed to the swelling of calcium silicate hydrate (C-S-H) when it interacts with water. The nonlinear behavior of the water absorption curve indicates that the sorptivity of concrete evolves during the water absorption process, largely due to the C-S-H gel swelling, which influences the permeability of the concrete.

A reduction in the water absorption rate was observed in the groups modified with silane integral modification (SI-M), silane surface modification (SS-M), and sodium silicate surface modification (S-M). These results clearly indicate that both surface modification of the recycled aggregates and cement matrix modification can effectively enhance the water resistance of RAC. Specifically, for the surface modification treatments using silane emulsion and sodium silicate, the modified recycled aggregates exhibited a lower water absorption rate compared to the unmodified aggregates. This improvement suggests that when the saturated recycled aggregates are used in the concrete preparation, less water is expelled from the modified aggregates during the mixing and curing stages. Consequently, a denser interfacial transition zone (ITZ) between the recycled aggregates and the new cement matrix is formed, contributing to improved water diffusion resistance in the RAC.

Among the various modification strategies, the group treated with sodium silicate surface modification (SS-M) demonstrated superior water resistance compared to the group treated with silane emulsion surface modification (S-M). This difference can be explained by two main factors. First, the reduction in water absorption of the recycled aggregates treated with silane emulsion (SS-M) was less significant than that of the aggregates treated with sodium silicate (S-M). This could be due to the application method: the spraying treatment used for silane emulsion may require more water to achieve surface saturation of the recycled aggregates, potentially leading to the formation of a relatively looser ITZ. Additionally, the hydrophobic film formed by the silane emulsion on the surface of the aggregates may negatively affect the hydration process in the ITZ, further contributing to the less compact microstructure observed in the silane-treated concrete.

Further investigation is needed to fully understand the influence of these modifications on the pore structure of the ITZ. In this study, backscattered electron imaging (BSE) combined with image processing technology was used to reveal the porosity characteristics of the ITZ, as discussed in the following section.

In addition to the surface modifications, incorporating silane emulsion directly into the cement matrix also improved the water diffusion resistance of the RAC. The hydrophobization effect induced by the silane emulsion reduces both the rate and overall amount of water absorption by decreasing the capillary forces within the modified concrete. However, it should be noted that the SI-M treatment (silane integral modification) did not provide the same level of water resistance as the S-M and SS-M treatments. This discrepancy is likely due to the reduced degree of cement hydration in the SI-M group, where the incorporation of silane emulsion into the cement matrix impairs the hydration process. As a result, the compactness and overall density of the concrete modified with silane integral modification were not as desirable as those observed in the SS-M and S-M groups.

To further explore the hydration degree of cement pastes with and without silane modification, an analysis of the hydration kinetics and microstructural development of the cement matrix was conducted in the following section. These findings will provide additional insight into the effectiveness of the various modification techniques in enhancing the water resistance and overall durability of RAC.
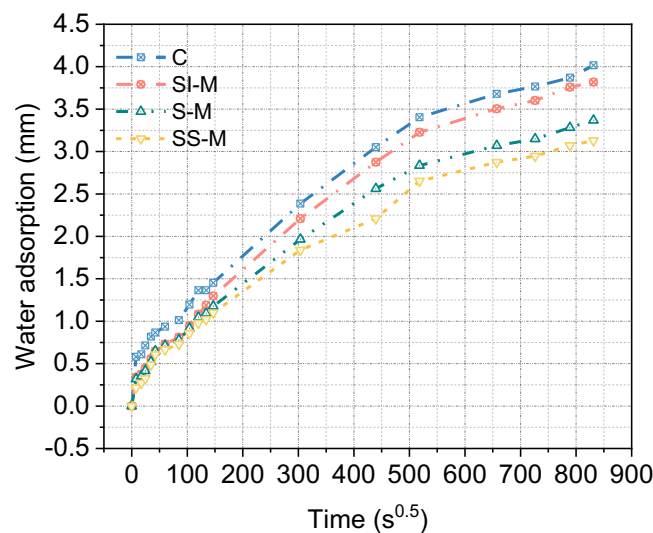
Fig.9 Water absorption of RAC

Mechanical properties and freeze-thaw resistance

Figure 10 presents the compressive and flexural strengths of recycled aggregate concrete (RAC) with and without modifications. Initially, the compressive and flexural strengths of the control group were recorded at 14.2 MPa and 4.83 MPa, respectively. Notably, a significant improvement in both compressive and flexural strengths was observed in the groups subjected to surface modifications, particularly in the sodium silicate-modified (SS-M) and silane-modified (S-M) groups. This enhancement in mechanical performance can be attributed to the surface modification of the recycled aggregates (RA), which led to a reduction in the water absorption capacity of the RA. As a result, less water was required to saturate the surface of the RA, thereby decreasing the overall water content and improving the integrity of the interfacial transition zone (ITZ) between the RA and the new cement matrix.

The mechanical performance improvement observed in the SS-M group can be explained by the unique properties of sodium silicate. The sodium silicate treatment densified the RA by filling pores and micro-cracks with a polymerized silicate gel. This gel also reacted with residual calcium hydroxide [$Ca(OH)_2$], forming additional calcium silicate hydrate (C-S-H) gel, which further strengthened the structure of the RA. During the drying process, the generated C-S-H gel reacted with carbon dioxide (CO_2) to form calcium carbonate ($CaCO_3$), which coated the surface of the treated RA. These processes reduced the water absorption of the RA and contributed to the formation of a denser ITZ, enhancing both the compressive and flexural strengths.

It is noteworthy that the SS-M group exhibited the greatest strength improvement. The compressive and flexural strengths of the SS-M specimens reached 18 MPa and 5.6 MPa, respectively. In comparison, the S-M group achieved compressive and flexural strengths of 16.8 MPa and 5.33 MPa. This variation in strength enhancement can be attributed to differences in the ITZ created by the surface modifications. In the S-M group, the silane emulsion formed a hydrophobic film on the surface of the RA, which resulted in a relatively weaker bond between the RA and the cement matrix compared to the SS-M group. This weaker bond likely hindered the hydration process within the ITZ, resulting in a slightly inferior mechanical performance.

Conversely, the silane integral modification (SIM) group demonstrated the lowest initial compressive and flexural strengths, recorded at 13.4 MPa and 4.33 MPa, respectively. This initial strength reduction is likely due to the lower degree of cement hydration caused by the incorporation of silane emulsion into the cement matrix, as will be discussed in a subsequent section.

Regarding the impact of freeze-thaw damage on compressive and flexural strengths, all groups experienced a decline in strength as the freeze-thaw cycles progressed. The control group exhibited the most rapid rate of deterioration, with the compressive strength decreasing to 7.89 MPa after 140 freeze-thaw cycles, representing a reduction of 44.8%. The flexural strength degradation was even more pronounced, with the residual flexural strength of the control group falling to 1.96 MPa after 140 cycles, a 51% reduction.

In contrast, the modified groups exhibited significantly better resistance to freeze-thaw damage. The reduction in compressive strength after 140 cycles for the SS-M, S-M, and SIM groups was limited to 17%, 18%, and 23%, respectively. A similar trend was observed in flexural strength, with the residual flexural strengths of the SS-M, S-M, and SIM groups recorded at 4.47 MPa, 4.11 MPa, and 3.09 MPa, respectively.

It is important to note that while the SIM treatment improved freeze-thaw resistance, it came at the cost of reduced initial strength. However, this initial deficiency could potentially be mitigated through adjustments to the water-to-binder ratio or by incorporating supplementary materials such as silica fume or fly ash. These strategies could enhance the mechanical performance while maintaining the durability benefits offered by the silane integral modification.
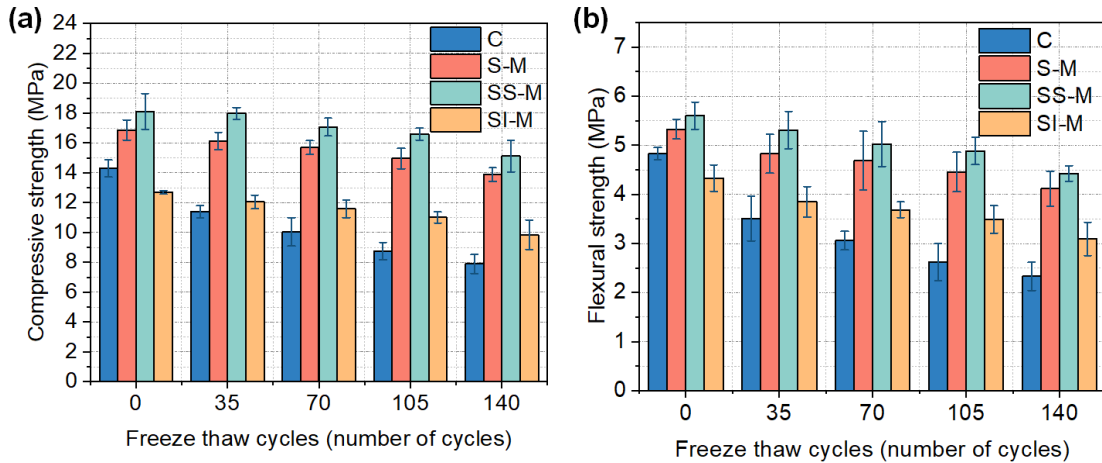
Fig.10 Mechanical performance of RAC; (a) Compressive strength of modified and unmodified RAC; (b) Flexural strength of modified and unmodified RAC

The mass loss ratio and relative dynamic elastic modulus (RDEM) of samples subjected to freeze-thaw damage are presented in Figure 11. The results clearly demonstrate that all three modifications—silane surface modification (SS-M), sodium silicate surface modification (S-M), and silane integral modification (SIM)—significantly enhance the freeze-thaw durability of recycled aggregate concrete (RAC). The modified concrete samples exhibited lower mass loss ratios and higher RDEM values compared to the control group (C).

After 70 freeze-thaw cycles, the mass loss ratio for the control group was 4.97%, which is indicative of imminent failure. In contrast, the mass loss ratio for the SIM group was considerably lower at 1.89%. Even lower mass loss ratios were observed in the SS-M and S-M groups, with values of 1.24% and 1.58%, respectively. These findings illustrate the improved durability conferred by the surface and integral modifications.

The trend continued as the number of freeze-thaw cycles increased. After 240 cycles, the control group showed a substantial mass loss ratio of 29.51%, accompanied by significant surface spalling, as depicted in Figure 11. In contrast, the SIM group exhibited a mass loss ratio of 19.58%, while the S-M group fared even better, with a mass loss ratio of 13.26%. The SS-M group demonstrated the best freeze-thaw resistance, with a notably lower mass loss ratio of 10.36%.

One important observation is the accelerated deterioration rate of the SIM group after 140 cycles. This suggests that the initial improvement in freeze-thaw resistance achieved through silane cement matrix modification begins to diminish with successive freeze-thaw cycles. The generation of cracks during freeze-thaw cycles is primarily driven by hydraulic pressures within the pores that exceed the material's tensile strength. This crack formation is influenced by both the capillary forces and the overall matrix strength. While the incorporation of silane emulsion in the cement matrix reduces capillary forces and slows water diffusion, it also weakens the cement matrix, which may explain the reduced long-term freeze-thaw resistance observed in the SIM group.

A similar trend was observed in the relative dynamic elastic modulus (RDEM). The control group experienced a rapid decline in RDEM with increasing freeze-thaw cycles, dropping below 60% after 80 cycles, signifying specimen failure. In contrast, the SS-M, SIM, and S-M groups displayed enhanced

resistance to freeze-thaw damage. The SIM group maintained its integrity until after 140 cycles, while the S-M group endured up to 180 cycles before failure. The SS-M group exhibited the longest freeze-thaw resistance life, sustaining around 180 cycles before any significant degradation.

These findings underscore the effectiveness of the surface and matrix modifications in enhancing the freeze-thaw resistance of RAC. Among the modified groups, SS-M demonstrated the best overall performance, exhibiting the lowest mass loss and highest RDEM values across the freeze-thaw cycles. This superior performance can be attributed to the densification of the ITZ and the formation of a robust protective layer on the recycled aggregates, which collectively contribute to the enhanced freeze-thaw durability of the concrete.

In conclusion, the macroscopic investigations affirm that SS-M, SIM, and S-M modifications all contribute to improving the freeze-thaw resistance of RAC, with SS-M showing the most substantial enhancement. The differences in performance between the modifications can be linked to their respective impacts on the ITZ, capillary forces, and overall matrix strength, which are critical factors in determining the freeze-thaw durability of RAC.
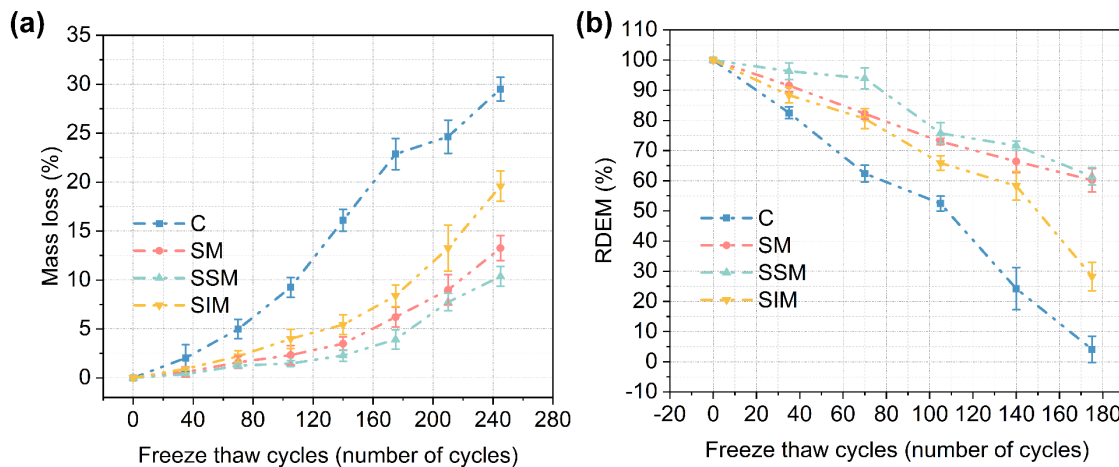

Fig. 11 Freeze-thaw resistance of modified and unmodified RAC; (a) mass loss ratio; (b) RDEM

Findings on miscoscale investigation on recycled aggregate concrete with different modifications

Morphology of the recycled aggregate surface

In the silane emulsion surface modification process, recycled aggregates (RA) were treated by spraying them with a diluted triethoxyoctylsilane emulsion. Scanning electron microscopy (SEM) images (Fig. 12(a) and (b)) revealed distinct differences in the surface morphology between untreated and treated RA. The untreated RA displayed a porous and rough surface, while the treated RA was coated with a continuous hydrophobic membrane. The chemical bonding mechanism underlying this modification can be described as follows: first, the ethoxyl groups of triethoxyoctylsilane undergo hydrolysis, forming hydroxyl groups in the alkaline environment provided by the RA. Subsequently, a condensation reaction occurs, leading to the formation of Si-O-Si bonds. As the treated aggregates dry, moisture evaporates, and a hydrophobic silicone-based film forms on the surface of the RA (Fig. 12(b)). This membrane plays a critical role in reducing the water absorption capacity of the RA, which is essential for improving the performance and durability of recycled aggregate concrete (RAC) under environmental stressors such as freeze-thaw cycles.

The sodium silicate surface modification operates via a different mechanism. When sodium silicate is dissolved in water, it undergoes hydrolysis, which can be represented by the following chemical equation (Eq. 5). The dissolved sodium silicate particles migrate and concentrate on the surface of the RA, filling micro-cracks and pores, thereby increasing the compactness and reducing the porosity of the aggregates. This densification occurs through the formation of a highly polymerized networked silicate gel, which not only fills surface irregularities but also penetrates deeper into micro-cracks and voids within the RA. Additionally, the silicate ions present in the solution react with the residual calcium hydroxide [$Ca(OH)_2$] on the RA surface to generate calcium silicate hydrate (C-S-H) gel, which further strengthens the aggregates by reducing porosity.

During the drying phase of this treatment, a secondary reaction occurs, where the newly formed C-S-H gel reacts with atmospheric carbon dioxide (CO_2) to produce calcium carbonate ($CaCO_3$). This $CaCO_3$ layer covers the surface of the treated RA, contributing to further densification and enhancing the durability of the aggregates. This densification process significantly reduces the water absorption capacity of the RA, making it less susceptible to moisture ingress and the detrimental effects of freeze-thaw cycles. Figure 13 illustrates the densified structure of the RA after sodium silicate treatment, highlighting the improvement in the surface texture and the closure of pores and cracks.

Both silane and sodium silicate modifications have been shown to improve the performance of RAC by reducing water absorption and enhancing the structural integrity of the interfacial transition zone (ITZ)

CIAMTIS
U.S. DOT Region 3 University Transportation Center

between the RA and the new cement matrix. By reducing water penetration, these treatments mitigate the weakening of the ITZ, which is typically a vulnerable area in RAC due to the inherent properties of recycled aggregates. Consequently, the improved ITZ leads to enhanced durability and mechanical performance, particularly in environments subject to freeze-thaw cycles and other durability challenges. These chemical treatments, through the formation of protective layers and densified microstructures, contribute to the long-term sustainability and performance of recycled aggregates in concrete applications.

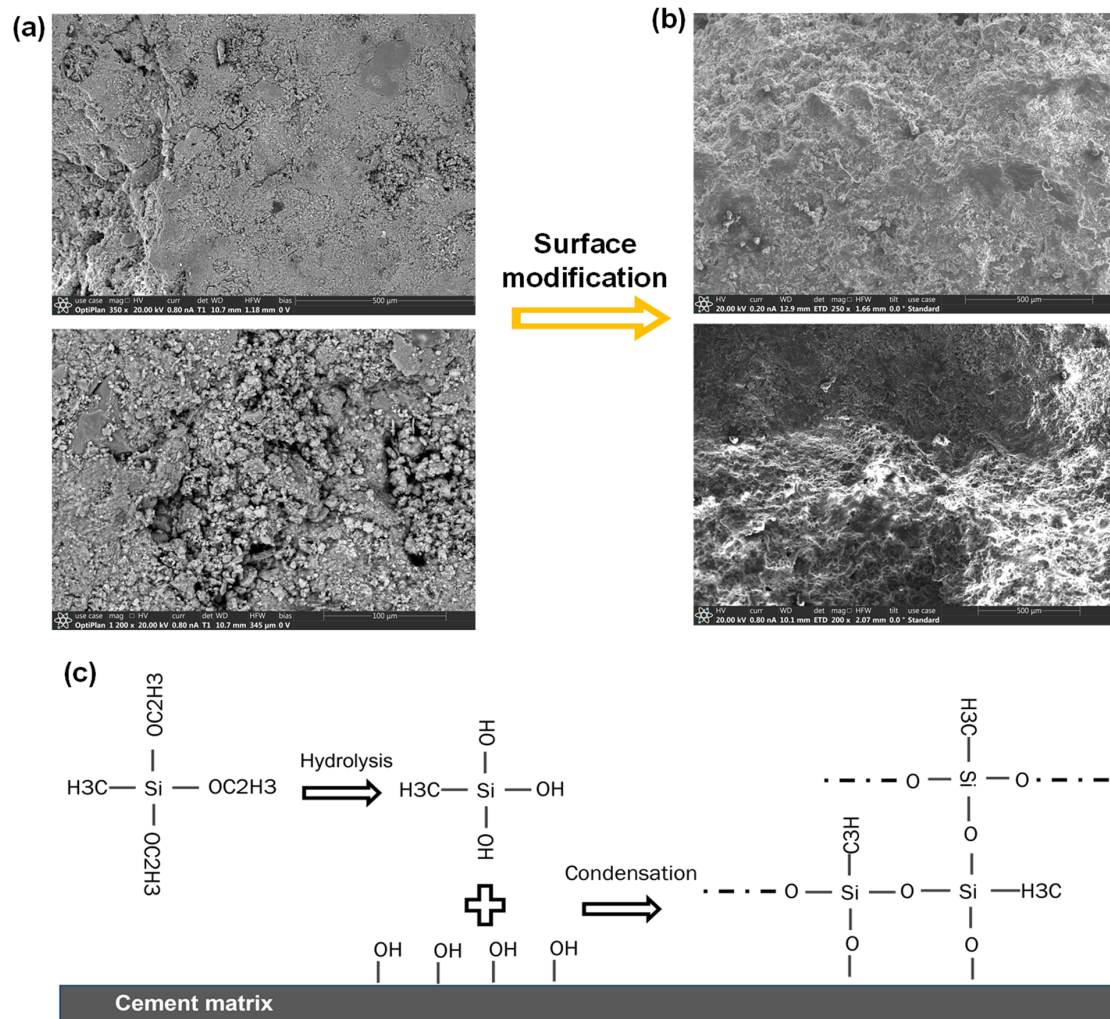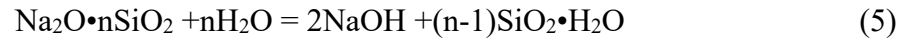$$Na_2O \bullet nSiO_2 + nH_2O = 2NaOH + (n-1)SiO_2 \bullet H_2O \qquad (5)$$

Fig. 12 The silane emulsion surface modification; (a) surface of unmodified RCA; (b) surface of modified RCA; (c) the mechanism of silane emulsion surface modification
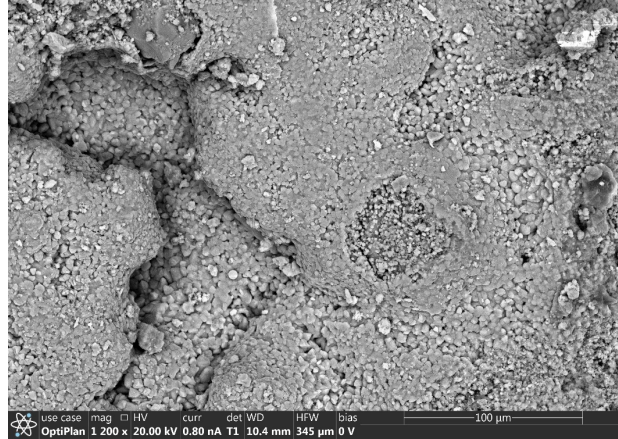
Fig. 13 The surface of RCA after sodium silicate modification

Cement hydration influenced by silane emulsion cement matrix modification

The effect of silane cement matrix modification on the hydration process of cement was analyzed using the backscattered electron image analysis (BSE-IA) method. A total of 10 BSE images were used to assess the control group and the silane-modified cement matrix group. The distributions of unhydrated cement and porosity are illustrated in Figure 14. The results indicated that the average proportion of unhydrated cement in the control group was 12.1%, whereas in the silane-modified group, it increased to 17.4%. This significant difference highlights the reason for the observed reduction in strength in the silane-modified cement matrix: the incorporation of silane emulsion limits the hydration of cement particles.

The presence of a hydrophobic silicone membrane, formed as a result of the silane modification, prevents water from reaching the cement particles, thereby reducing the hydration degree. The reduction in hydration negatively affects the development of the cement matrix's mechanical properties, contributing to lower overall strength.

In addition to the reduced hydration degree, the porosity of the modified cement paste was found to be higher than that of the unmodified cement paste. Specifically, the modified cement paste exhibited a porosity of 9.63%, compared to 6.75% in the unmodified cement paste. This increased porosity further corroborates the finding that the incorporation of silane emulsion into the cement matrix limits cement hydration, resulting in a less dense and more porous microstructure. This increased porosity compromises the mechanical strength of the cement matrix, as it introduces more voids and weak points within the structure.

In summary, the BSE-IA analysis clearly demonstrates that the silane modification of the cement matrix results in a reduced degree of cement hydration and an increase in porosity, both of which contribute to the observed strength reduction in the modified concrete. These findings highlight the trade-offs associated with silane modification, as the enhanced water resistance comes at the cost of reduced mechanical performance.
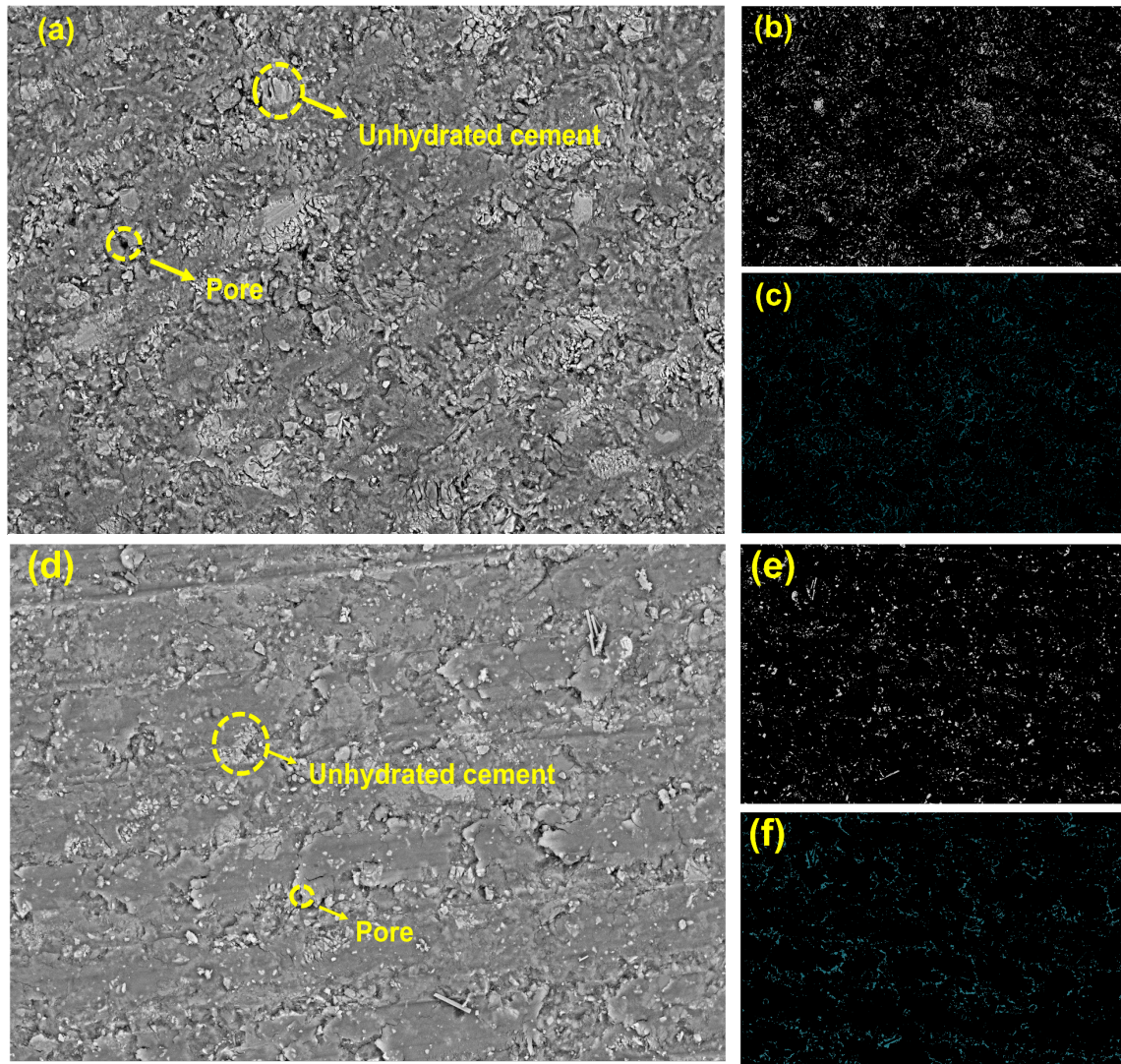
Fig.14 BSE analysis of cement paste with and without silane emulsion internal modification (a) a typical BSE of cement paste; (b) the distribution of anhydrous cement in cement paste; (c) the distribution of porosity in cement paste; (d) a typical BSE of cement paste with silane emulsion internal modification; (e) the distribution of anhydrous cement in modified cement paste; (f) the distribution of porosity in modified cement paste.

Porosity of interfacial transition zone

The interfacial transition zone (ITZ) between recycled aggregate (RA) and the newly formed cement matrix was analyzed using the Backscattered Electron Image Analysis (BSE-IA) method, incorporating 25 BSE images from all experimental groups. Representative images are provided in Figure 17, and the mean porosity of the ITZ, as a function of distance from the RA interface, is presented in the same figure. Among the tested groups, the ITZ associated with the sodium silicate-modified (SS-M) RA exhibited the lowest porosity, indicating the most compact structure, while the silane-modified (SI-M) RA showed the highest porosity. The ITZ in the surface-modified RA (S-M) group demonstrated a lower porosity than that of the unmodified control group. These findings clearly indicate that surface modifications

U.S. DOT Region 3 University Transportation Center

significantly improve ITZ compactness, with sodium silicate surface modification yielding the most substantial enhancements.

A key factor contributing to this improvement is the ability of surface modifications to mitigate the water accumulation at the RA-cement interface. In the unmodified control group, recycled aggregates (RA) in a saturated-surface-dry (SSD) state contain a significant amount of free water, both within the RA and in the surrounding cement paste. During the mixing and curing processes, this excess water tends to concentrate at the RA-cement interface, promoting the formation of larger hydration products, such as ettringite and calcium hydroxide, in the ITZ. This results in increased porosity and a weakened bond between the RA and the new cement matrix.

In contrast, sodium silicate surface modification reduces the water absorption capacity of RA, which limits the availability of free water at the interface during mixing and curing. As a result, a denser ITZ structure is formed, with more calcium silicate hydrate (C-S-H) gel and fewer large hydration crystals. This leads to a stronger bond and lower porosity in the ITZ. Additionally, the presence of sodium silicate promotes the hydration process in the surrounding cement paste, further enhancing the compactness and mechanical performance of the ITZ.

Silane surface modification also improves ITZ properties, though its impact is slightly less pronounced compared to sodium silicate modification. The hydrophobic silicone film created by the silane emulsion prevents water accumulation at the RA-cement interface, resulting in a denser ITZ structure. However, the difference in water absorption between RA treated with silane and sodium silicate can explain the varying degrees of ITZ enhancement. As demonstrated in previous studies, RA modified with sodium silicate has a lower water absorption rate than RA modified with silane emulsion, which leads to a more effective reduction in ITZ porosity. Moreover, the presence of silane emulsion negatively affects the hydration process within the ITZ, further limiting its compactness.

These findings highlight that the ITZ plays a crucial role in the overall performance of RAC, and surface modification techniques can significantly enhance freeze-thaw resistance and mechanical properties by improving the ITZ structure. Among the modifications studied, sodium silicate surface modification (SS-M) provided the greatest improvement in ITZ properties, which correlates with the best freeze-thaw resistance and mechanical performance observed in this group.
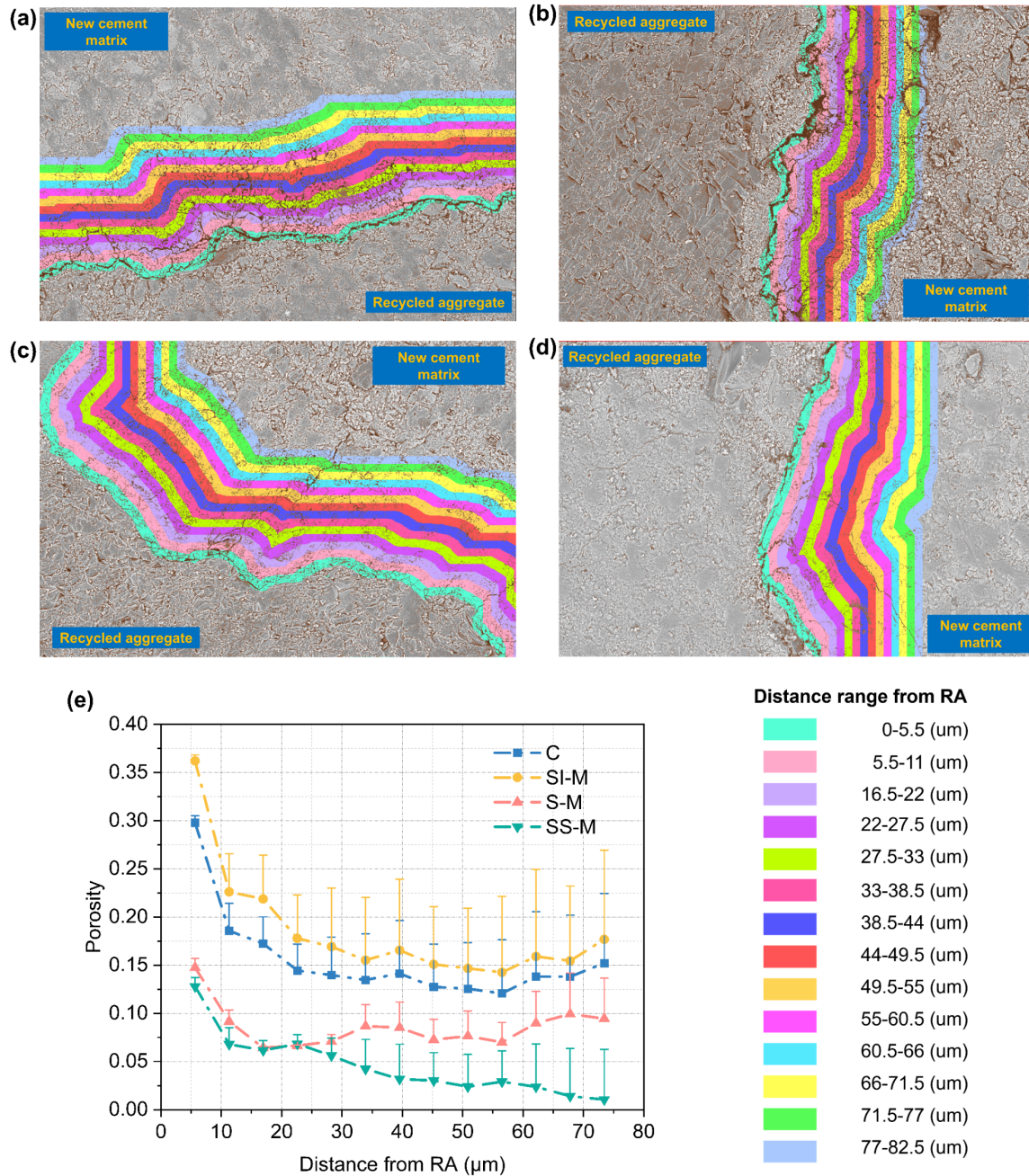
Fig.15 ITZ analysis of RAC with and without modifications; (a) ITZ of C; (b) ITZ of SI-M; (c) ITZ of S-M; (d) ITZ of SS-M; (e) the summary of the porosity vs distance from RA

CHAPTER 5

Findings on fatigue behavior investigation on recycled aggregate concrete with different modifications

The fatigue life under freeze-thaw damage

Tables 4-7 present the fatigue life characteristics of concrete specimens—denoted as Control (C), Sodium Silicate Surface Modification (SS-M), Silane Surface Modification (S-M), and Silane Integral Modification (SI-M)—under varying freeze-thaw cycles (0, 70, and 140 cycles). The stress levels analyzed are 0.8, 0.7, and 0.6. The data reveal an inverse relationship between fatigue life and stress level, as higher stress levels consistently result in shorter fatigue life within the same group and freeze-thaw conditions. As the number of freeze-thaw cycles increases, the fatigue life of recycled aggregate concrete (RAC) declines, with the control group exhibiting the most rapid deterioration.

The results also show substantial variation in fatigue life among the different groups under the same stress levels and freeze-thaw conditions. This variation can be attributed to several factors. Firstly, recycled aggregates (RA) have a heterogeneous composition compared to natural aggregates, often containing broken bricks, various types of crushed concrete, and differing amounts of aged cement paste or mortar. These inconsistencies in RA composition significantly affect the fatigue characteristics of concrete made with recycled aggregates.

Secondly, the random distribution of RAs within the concrete, particularly in the tensile zone of beams used for fatigue testing, can contribute to variations in fatigue behavior. If weaker RAs are concentrated in the tensile zone, the fatigue performance may be adversely affected. Additionally, even under identical stress levels, the flexural strength of RAC is influenced by the properties of the RAs, leading to significant differences in fatigue life across samples.

To ensure the accuracy of the fatigue life data, the Chauvenet criterion was applied to evaluate and exclude potential outliers [38]. The fatigue life data was first logarithmically transformed, and the mean and standard deviation were calculated for standardization. For groups with five samples, the Chauvenet limit value was determined to be 1.645. Any standardized fatigue life value exceeding this limit would be considered an outlier and excluded from further analysis. The standardization process for fatigue life is outlined in Eq. (6). Notably, all specimens in this study had fatigue life values below the Chauvenet limit, confirming that none of the data points were outliers and thus suitable for further fatigue analysis.

This process ensures that the variability observed in fatigue life among the different groups can be reliably attributed to the inherent properties of the RAs and the effects of freeze-thaw damage, rather than inconsistencies or anomalies in the data.

$$Nor(\lg N) = \left| \frac{\lg N - Ave(\lg N)}{Std(\lg N)} \right| \qquad (6)$$

Where Nor-Standardized values; Ave-Arithmetic mean; Std-Standard deviation.

Table.4 Flexural fatigue life of C and Chauvenet assessment

F-T	Stress-level	N	lgN	Ave (lgN)	Std (lgN)	Nor (lgN)
0	0.8	3560	3.551	3.678	0.104	1.207
		4687	3.671			0.064
		5788	3.763			0.814
		6305	3.800			1.170
	0.7	10780	4.033	4.277	0.146	0.712
		20394	4.310			1.681
		19883	4.298			0.221
		26501	4.423			0.146
		70560	4.849			1.003
	0.6	54687	4.738	4.685	0.163	0.312
		63788	4.805			1.003
		37305	4.572			0.324
		28982	4.462			0.734
70	0.8	2889	3.461	3.326	0.168	0.805
		3187	3.503			1.059
		2066	3.315			0.062
		1208	3.082			1.451
		1848	3.267			0.351
	0.7	8795	3.944	3.976	0.181	0.173
		15589	4.193			1.200
		12910	4.114			0.762
		7746	3.889			0.478
		5475	3.738			1.311
	0.6	28587	4.456	4.417	0.154	0.257
		16364	4.214			1.314
		40005	4.602			1.204
		20458	4.311			0.685
		31587	4.500			0.538
140	0.8	712	2.852	2.859	0.152	0.041
		815	2.911			0.345
		1201	3.080			1.451
		471	2.673			1.220
		599	2.777			0.534
		2100	3.322			1.496
	0.7	4254	3.629	3.596	0.183	0.177
		3322	3.521			0.409
		5259	3.721			0.679
		6145	3.789			1.049
	0.6	22899	4.360	4.195	0.155	1.065
		9843	3.993			1.302
		19899	4.299			0.672

| | | 17687 | 4.248 | | | 0.341 |
| | | 11874 | 4.074 | | | 0.777 |

Table.5 Flexural fatigue life of S-M and Chauvenet assessment

F-T	Stress-level	N	lgN	Ave (lgN)	Std (lgN)	Nor(lgN)
0	0.8	52293	4.718			1.320
		62000	4.792	4.874	0.118	0.694
		78975	4.897			0.197
		101375	5.006			1.116
	0.7	90568	4.957			0.701
		286036	5.456	5.480	0.145	0.166
		324568	5.511			0.212
		378979	5.579			0.677
	0.6	175556	5.244			1.628
		408987	5.612			0.905
		578957	5.763	5.910	0.147	1.004
		839997	5.924			0.098
		1265896	6.102			1.313
70	0.8	70568	4.849			1.477
		34123	4.533			1.380
		49876	4.698	4.686	0.110	0.112
		55879	4.747			0.559
		39877	4.601			0.768
	0.7	289546	5.462			1.363
		163338	5.213			0.898
		159587	5.203	5.312	0.110	0.990
		266980	5.426			1.043
		179877	5.255			0.517
	0.6	621687	5.794			0.385
		804567	5.906			1.486
		586879	5.769	5.755	0.156	0.138
		394899	5.596			1.555
		510817	5.708			0.455
140	0.8	32212	4.508			0.037
		50568	4.704			1.333
		28898	4.461	4.513	0.143	0.367
		19145	4.282			1.617
		40887	4.612			0.687
	0.7	129568	5.112			1.094
		137969	5.140			0.742
		202956	5.307	5.198	0.098	1.419
		142778	5.155			0.550
		187245	5.272			0.968
	0.6	353314	5.548			0.676
		248792	5.396			1.614
		556781	5.746	5.658	0.162	0.542
		690120	5.839			1.116
		575891	5.760			0.632

U.S. DOT Region 3 University Transportation Center

Table.6 Flexural fatigue life of SS-M and Chauvenet assessment

F-T	Stress-level	N	lgN	Ave (lgN)	Std (lgN)	Nor (lgN)
0	0.8	166320	5.221	5.191	0.100	0.298
		158877	5.201			0.099
		208650	5.319			1.280
		148800	5.173			0.184
		110010	5.041			1.493
	0.7	576888	5.761	5.803	0.120	0.348
		617891	5.791			0.100
		429859	5.633			1.408
		758935	5.880			0.641
		889833	5.949			1.215
	0.6	1699852	6.230	6.203	0.119	0.232
		1358995	6.133			0.588
		1858987	6.269			0.559
70	0.8	108645	5.036	5.013	0.113	0.201
		135894	5.133			1.062
		99467	4.998			0.138
		67894	4.832			1.607
		116889	5.068			0.482
	0.7	518569	5.715	5.642	0.141	0.521
		334589	5.525			0.832
		658856	5.819			1.260
		472231	5.674			0.232
		298756	5.475			1.181
		1201153	6.080			0.091
	0.6	831213	5.920	6.068	0.130	1.139
		946578	5.976			0.705
		1278951	6.107			0.301
		1804678	6.256			1.452
140	0.8	101144	5.005	4.882	0.121	1.021
		70346	4.847			0.285
		90789	4.958			0.633
		49332	4.693			1.561
		80325	4.905			0.192
	0.7	356641	5.552	5.536	0.168	0.095
		195677	5.292			1.453
		459895	5.663			0.750
		288789	5.461			0.449
		517894	5.714			1.057
		859456	5.934			0.173
		1268971	6.103			1.114
	0.6	965678	5.985	5.903	0.180	0.455
		747861	5.874			0.162
		415678	5.619			1.580

Table.7 Flexural fatigue life of SI-M and Chauvenet assessment

F-T	Stress-level	N	lgN	Ave (lgN)	Std (lgN)	Nor (lgN)
0	0.8	3005	3.478	3.536	0.081	0.298
		2785	3.445			0.099
		3958	3.597			1.280
		3156	3.499			0.184
	0.7	4598	3.663	4.179	0.099	1.493
		14852	4.172			0.348
		21692	4.336			0.100
		16596	4.220			1.408
		13528	4.131			0.641
	0.6	10887	4.037	4.565	0.113	1.215
		35296	4.548			0.232
		53968	4.732			0.588
		34197	4.534			0.559
70	0.8	1589	3.201	3.259	0.117	0.201
		1637	3.214			1.062
		1401	3.146			0.138
		2811	3.449			1.607
		1927	3.285			0.482
	0.7	5789	3.763	3.930	0.136	0.521
		9989	4.000			0.832
		12900	4.111			1.260
		8658	3.937			0.232
		6901	3.839			1.181
	0.6	34587	4.539	4.370	0.163	0.091
		25864	4.413			1.139
		30004	4.477			0.705
		13457	4.129			0.301
		19587	4.292			1.452
140	0.8	907	2.958	3.062	0.204	1.021
		1744	3.242			0.285
		589	2.770			0.633
		1804	3.256			1.561
		1209	3.082			0.192
	0.7	3457	3.539	3.655	0.131	0.095
		6711	3.827			1.453
		3265	3.514			0.750
		4589	3.662			0.449
		5414	3.734			1.057
	0.6	13899	4.143	4.268	0.110	0.173
		17845	4.252			1.114
		15899	4.201			0.455
		26687	4.426			0.162
		20871	4.320			1.580

S-N curves

The stress level-fatigue life (S-N) curve is a crucial indicator for evaluating the fatigue performance of materials, providing valuable insights into their long-term behavior under varying stress levels. For concrete materials, the fatigue life is commonly expressed using a double natural logarithmic formulation, which allows for a more accurate representation of the relationship between stress levels and fatigue life across a wide range of conditions. This formulation can be mathematically represented as:

$$\ln S = b\ln N - a \tag{7}$$

Where S refers to the stress level, and N is the flexural fatigue life, a is the intercept, b stands for how sensitive fatigue life is to changes in stress levels. The S-N curve derived from this relationship provides a clear visualization of how the fatigue life of concrete, particularly recycled aggregate concrete (RAC), changes with different stress levels. By plotting the stress level on the x-axis and the number of cycles to failure on the y-axis (both on a logarithmic scale), the curve helps in understanding how concrete materials, modified or unmodified, behave under cyclic loading.

This double logarithmic model is especially useful in assessing the long-term durability of concrete, particularly in applications subjected to repeated loading, such as pavements, bridges, and other infrastructure elements. Additionally, it allows for a comparative analysis of different modification techniques, such as sodium silicate or silane surface modifications, in terms of their effectiveness in enhancing the fatigue life of RAC under various stress conditions.

Figure 16 presents the stress level-fatigue life (S-N) curves for recycled aggregate concrete (RAC) with various surface and matrix modifications applied to the recycled aggregates. Across all mixtures, a consistent trend is evident: as the stress levels increase, the fatigue life decreases, aligning with observations in existing literature [24-27]. Notably, the sodium silicate surface modification (SS-M) and silane surface modification (S-M) groups exhibited a significant enhancement in fatigue performance, particularly under freeze-thaw damage. This improvement can be primarily attributed to the modification of recycled aggregates (RA) and the subsequent improvement of the interfacial transition zone (ITZ), which play a critical role in extending the flexural fatigue life of RAC.

In contrast, the silane integral modification (SI-M) group showed a lower fatigue life compared to the control group (C), likely due to the reduced cement hydration caused by the addition of silane emulsion in the cement matrix. Despite this reduction, the SI-M group demonstrated a slower rate of deterioration under freeze-thaw cycles compared to the control group, indicating improved freeze-thaw resistance. This suggests that, while the initial fatigue life of SI-M may be lower, the addition of silane emulsion offers some protective benefits against freeze-thaw damage, particularly if cement hydration can be improved through supplementary cementitious materials or a lower water-to-binder ratio.

Table 8 provides the parameters for the fitted S-N curves, with R^2 values ranging from 0.856 to 0.92, confirming the reliability of the fitted models in predicting the flexural fatigue life of RAC with and without modifications. When examining the slope (b) of the S-N curves at 0 freeze-thaw cycles, some variations emerge. The S-M and SS-M groups exhibited a slight decrease in slope compared to the control group (C), indicating a reduced sensitivity of fatigue life to stress levels. This reduction in sensitivity can be attributed to the improvements in the ITZ and the surface modification of recycled aggregates, which reduce porosity and enhance the bond between the RA and the cement matrix. These modifications likely fill initial pores and cracks on the RA surface, decreasing the overall pore and crack density in the RAC, thereby reducing its sensitivity to fatigue-induced stress.

Conversely, the SI-M group displayed increased sensitivity of fatigue life to stress levels, which may be due to increased ITZ porosity and reduced cement hydration, as caused by the presence of silane emulsion in the matrix. As freeze-thaw cycles progress, a consistent decrease in slope is observed across all groups,

indicating an increasing sensitivity of fatigue life to stress levels. This phenomenon suggests that cumulative freeze-thaw damage makes the concrete more vulnerable to stress-induced fatigue.

Notably, after 140 freeze-thaw cycles, the control group exhibited the most pronounced sensitivity to stress levels, reflecting the severe damage it experienced under freeze-thaw conditions. This heightened sensitivity is likely due to the propagation of cracks and other defects caused by freeze-thaw cycles, which weaken the structural integrity of the concrete, making it more susceptible to fatigue failure under increasing stress.

In conclusion, while all groups showed a decrease in fatigue life with increasing stress levels and freeze-thaw cycles, the surface modifications—particularly SS-M—significantly improved the durability of RAC under such conditions, reducing its sensitivity to stress levels and enhancing its overall performance in environments prone to freeze-thaw damage.
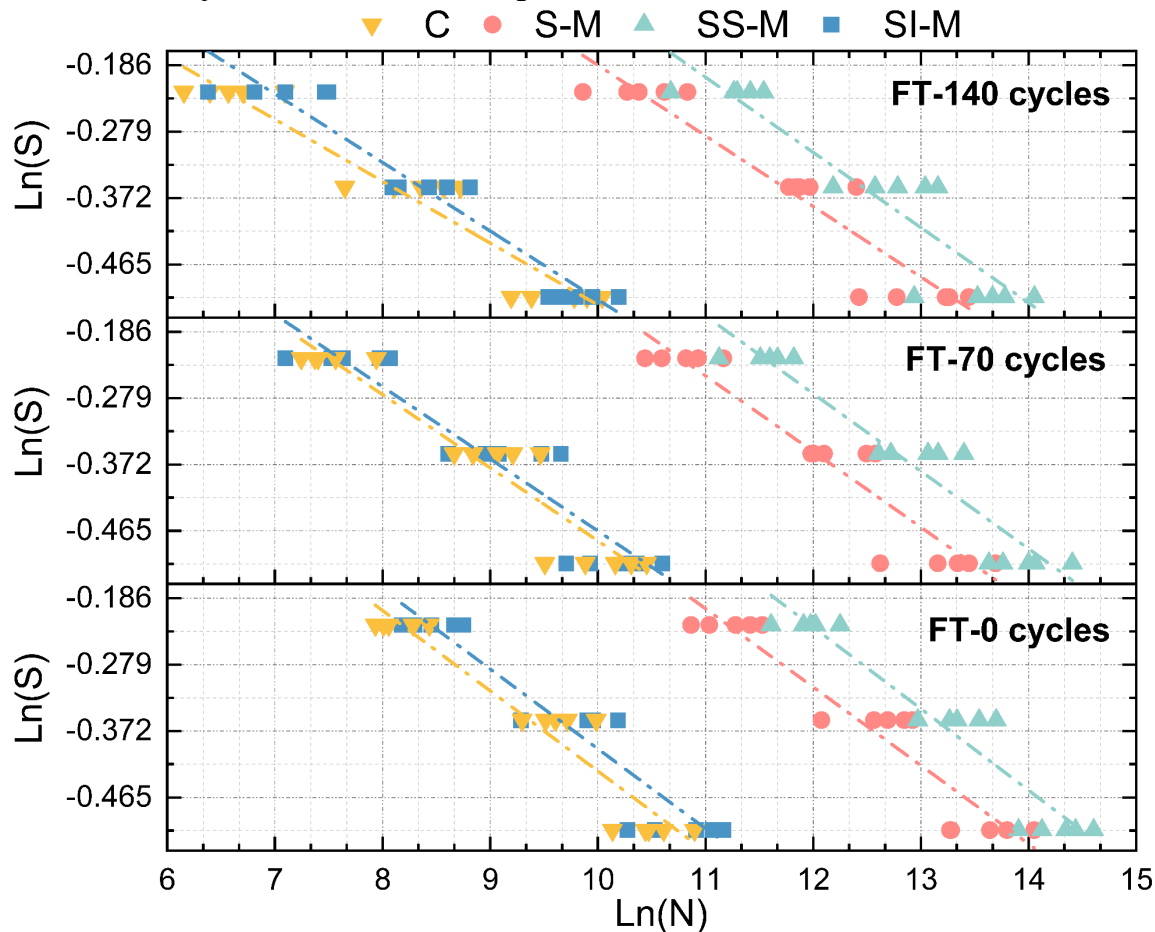

Fig. 16 The relationship between stress level and flexural fatigue life

It is recognized that, in real-world conditions, structural components are subjected to a wide range of variable stress levels rather than the discrete levels examined in this study. While this study focuses on three specific stress levels, the fitted equations presented in Figure 16 can be used to approximate the performance of structures under different stress conditions. These equations provide a reliable basis for predicting fatigue life across a broader range of stress levels, offering valuable insights into the long-term durability of recycled aggregate concrete (RAC) in real-world applications.

Table.8 Fitting parameters of S-N curves

Samples	Freeze-thaw cycle-0			Freeze-thaw cycle-70			Freeze-thaw cycle-140		
	a	b	R^2	a	b	R^2	a	b	R^2
C	0.721	-0.111	0.887	0.547	-0.101	0.869	0.345	-0.087	0.917
S-M	1.008	-0.112	0.898	0.921	-0.106	0.897	0.803	-0.099	0.892
SS-M	1.145	-0.112	0.913	1.034	-0.109	0.906	0.957	-0.105	0.844
SI-M	0.697	-0.110	0.913	0.547	-0.103	0.899	0.447	-0.096	0.921

The significance analysis of variables

In this section, the Kaplan-Meier (K-M) method, a nonparametric analysis, is employed to assess the impact of various modifications, freeze-thaw damage, and stress levels on the fatigue life of recycled aggregate concrete (RAC). Originally proposed by Kaplan and Meier in 1958, the K-M method is a widely used nonparametric survival analysis technique that does not require assumptions about the underlying distribution of fatigue life data [39]. The K-M survival curves visualize the cumulative survival rates, enabling a clear understanding of how different test variables affect fatigue life.

The specific steps of the K-M analysis in this study are as follows: each specimen's fatigue life is treated as a failure point, and if the specimen survives beyond this failure point, it is considered to have "survived." The proportion of surviving specimens relative to the total number of specimens at each failure point is used to calculate the cumulative survival rate, which is then plotted as survival curves to analyze the effects of stress levels, modifications, and freeze-thaw cycles on the fatigue life.

Figure 17 shows the survival curves illustrating the cumulative survival rates across various stress levels for the different experimental groups. In Figure 19(a), a clear trend emerges where increasing stress levels result in a significant decrease in fatigue life, accompanied by a steep decline in cumulative survival rates. The lack of overlap between the survival curves across stress levels indicates that stress levels have a marked impact on fatigue life. To further confirm the statistical significance of these differences, the Log-rank and Breslow tests were conducted, with results summarized in Table 9. Both tests yielded p-values far below 0.05, affirming the significant influence of stress levels on fatigue life.

Figure 17(b) displays survival curves for different modification treatments at varying stress levels. It is evident that surface treatments of the aggregates, such as sodium silicate and silane surface modifications, significantly enhance fatigue life and survival rates. Conversely, the silane integral modification negatively affects fatigue life and survival rates. These results highlight the substantial influence of different modification methods on fatigue performance. The Log-rank and Breslow tests, also summarized in Table 9, show test values well below 0.05, further validating the significant impact of these treatments on fatigue life.

In Figure 17(c), the Kaplan-Meier curves depict cumulative survival rates across different freeze-thaw cycles for all groups. While some overlap is observed between the survival curves, suggesting that the influence of freeze-thaw cycles on fatigue life may not be as strong as the effects of stress levels or

CIAMTIS
U.S. DOT Region 3 University Transportation Center

modification methods, the P-values show variability. This variability likely arises from the combined effects of freeze-thaw cycles, surface modifications, and stress levels, which together contribute to the observed differences in fatigue life.

In conclusion, the Kaplan-Meier method reveals that stress levels and modification methods significantly affect the fatigue life of RAC, as demonstrated by the cumulative survival rates and statistical tests. Although freeze-thaw cycles have an impact, their influence appears to be less pronounced compared to the other variables.
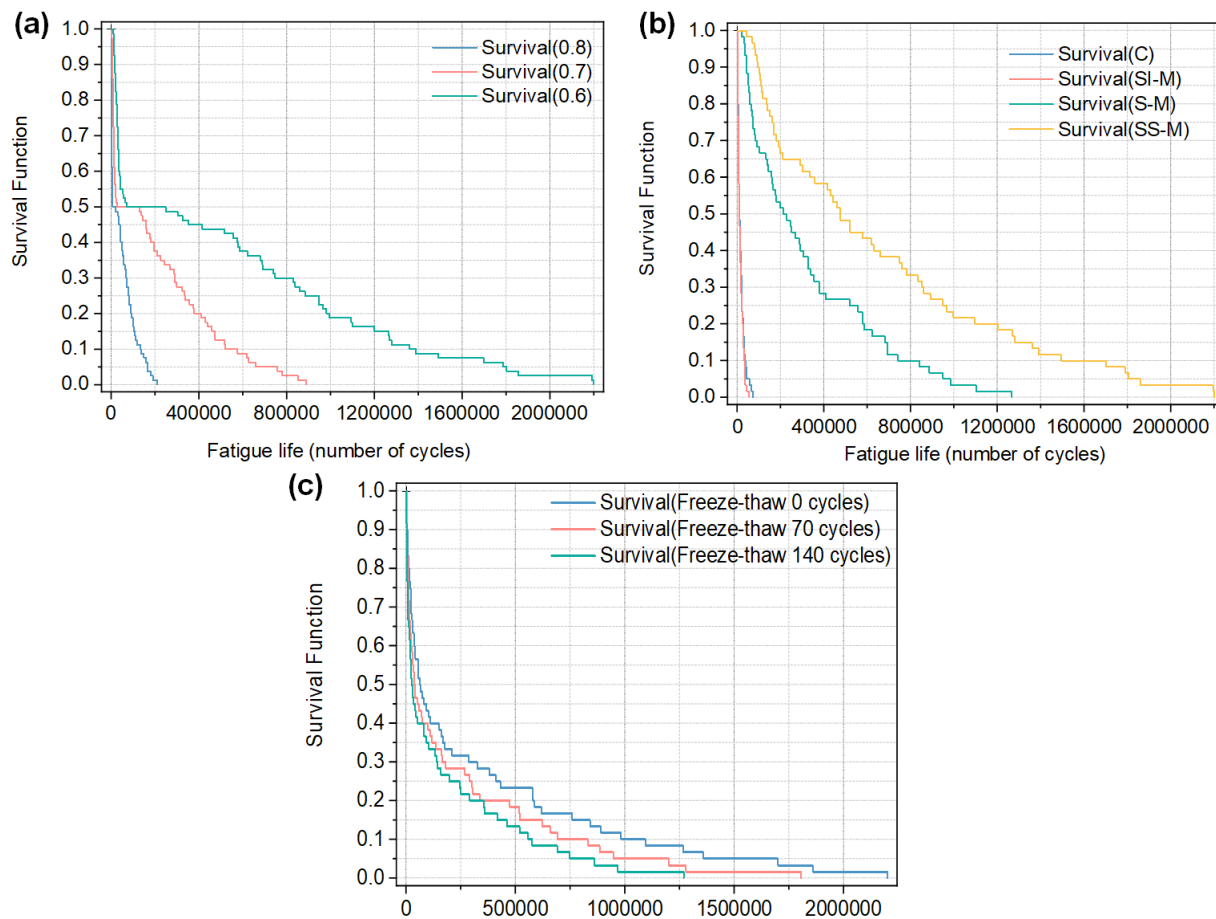

Fig. 17 The overall significance analysis of variables based on the Kaplan-Meier method; (a) Effect of stress level on K-M survival curve; (b) Effect of modifications on K-M survival curve; (c)Effect of freeze-thaw cycles on K-M survival curve.

Table.9 Test results of the significance analysis

	Stress level	Modifications	Freeze-thaw cycles
P value of Log-rank	<0.001	<0.001	0.05188
P value of Breslow	<0.001	<0.001	0.06479

To isolate and analyze the impact of freeze-thaw damage on flexural fatigue life, independent of stress levels and modification methods, Kaplan-Meier (K-M) analysis was applied to the fatigue life of samples from each modification group at a constant stress level of 0.8. The resulting survival curves are illustrated in Figure 18.

The outcomes of the Log-rank and Breslow tests, which are summarized in the analysis, indicate that freeze-thaw cycles have a significant effect on the flexural fatigue life of all concrete groups. The P-values consistently fall below 0.005, confirming the statistical significance of freeze-thaw cycles on the fatigue performance of recycled aggregate concrete (RAC). These findings demonstrate that, across all modification groups, the cumulative damage from freeze-thaw cycles plays a crucial role in diminishing the flexural fatigue life of RAC, further highlighting the importance of improving freeze-thaw resistance in concrete materials designed for durability in harsh environmental conditions.
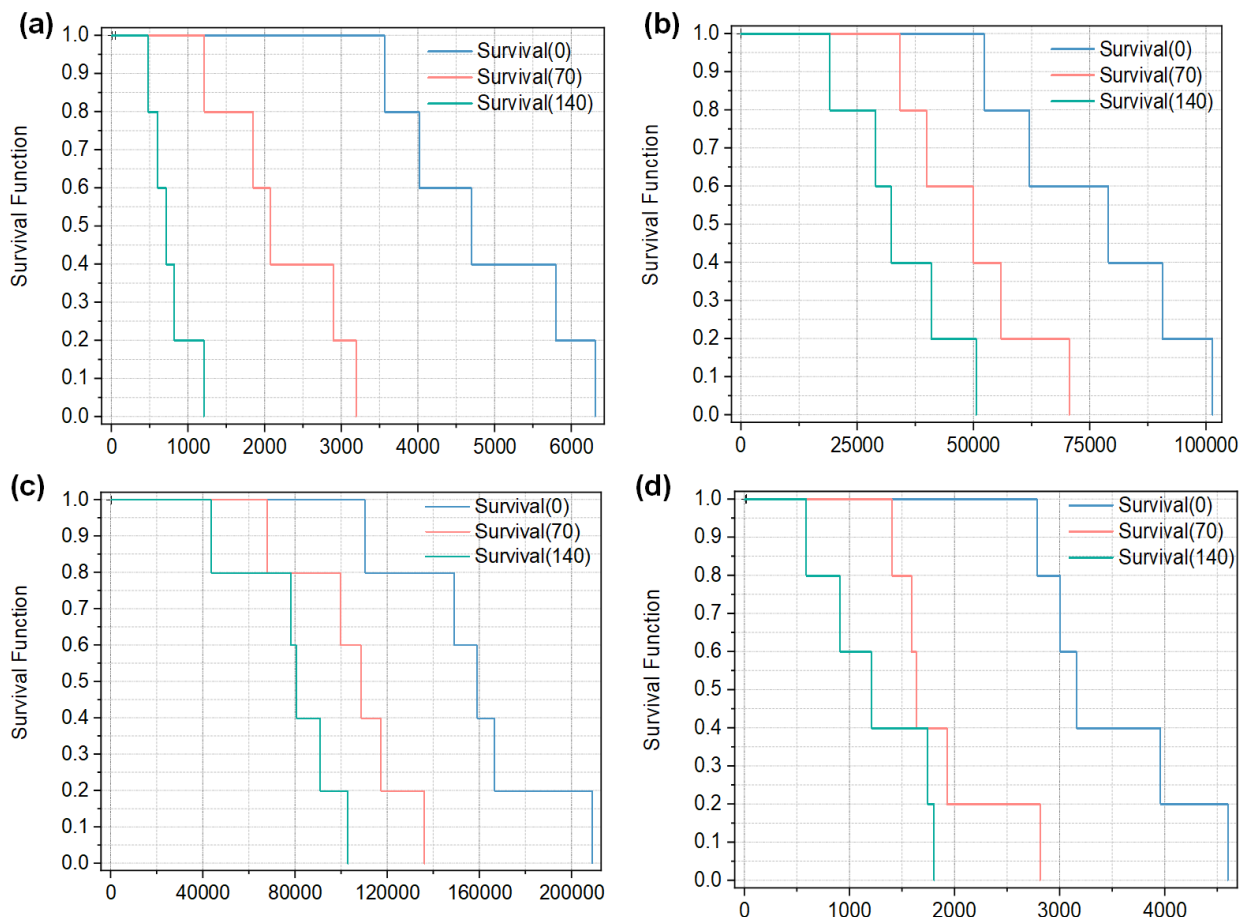

Fig.18 The significance analysis of freeze-thaw cycles of different groups with the stress level = 0.8based on K-M methods; (a) K-M curves of C; (b) K-M curves of S-M; (c) K-M curves of SS-M; (d) K-M curves of SI-M.

Table.10 Test results of the significance analysis (stress level=0.8)

Freeze-thaw cycles	C	S-M	SS-M	SI-M
P value of Log-rank	<0.001	0.00228	<0.001	0.0016
P value of Breslow	<0.001	0.00472	0.00373	0.00448

The distribution model of fatigue life

In this study, the Weibull two-parameter model is adopted to describe the fatigue life distribution of recycled aggregate concrete (RAC). The Weibull model is commonly used to characterize the fatigue life of concrete materials due to its ability to capture the probabilistic nature of material failure. This statistical model provides insights into various aspects of fatigue life, including probability distributions, probability density functions, reliability functions, and failure rates. These are mathematically expressed through the following key equations (Eqs. 8 to 10):

$$F(N) = 1 - \exp[-(\frac{N}{\lambda})^k] \tag{8}$$

$$f(N) = \frac{k}{\lambda} \times (\frac{N}{\lambda})^{k-1} \times 1 - \exp[-(\frac{N}{\lambda})^k] \tag{9}$$

$$R(N) = \exp[-(\frac{N}{\lambda})^k] \tag{10}$$

$$r(N) = \frac{f(N)}{R(N)} = \frac{k}{\lambda} \times (\frac{N}{\lambda})^{k-1} \tag{11}$$

Where: F(N) is the Weibull CDF; f(N) refers to Weibull PDF; R(N) stands for the Reliability function, r(N) is the Failure function; N is the number of cycles; k is the shape parameter; λ refers to the Dimensional parameters.

The parameters of the Weibull two-parameter model, specifically the scale parameter (η) and the shape parameter (β\beta$\beta$), are estimated using the maximum likelihood estimation (MLE) method. This statistical technique allows for the determination of the most likely values of these parameters, given the observed fatigue life data. The MLE process involves introducing the parameter ttt and defining it as t = λk where λ represents the failure rate and k is a constant associated with the likelihood function, and bringing it into Eq. 10 to get Eq. 12.

$$f(N) = \frac{k}{t} \times N^{k-1} \times \exp[-(\frac{N}{t})^k] \tag{12}$$

The likelihood function of the above equation is:

$$L(k,t \mid N_1, N_2 \ldots\ldots N_n) = \prod_{i=1}^{n} f(N_i \mid k,t) \tag{13}$$

Bring the Eq.12 to 13 can have:

$$L(k,t \mid N_1, N_2 \ldots \ldots N_n) = \left(\frac{k}{t}\right)^n \prod_{i=1}^{n} N_i^{k-1} \exp[-\frac{1}{t}\sum_{i=1}^{n} N_i^k] \tag{14}$$

Take the logarithm of both sides of Eq.14:

$$Ln(L(k,t \mid N_1, N_2 \ldots \ldots N_n)) = n(\ln k - \ln t) + (k-1)\sum_{i=1}^{n} \ln N_i - \frac{1}{t}\sum_{i=1}^{n} N_i^k \tag{15}$$

The partial derivatives of the parameters k and t are obtained by solving Eq. 15:

$$t = \frac{1}{n}\sum_{i=1}^{n} N_i^k \tag{16}$$

$$\frac{\sum_{i=1}^{n} \ln N_i^k \ln N_i}{\sum_{i=1}^{n} N_i^k} - \frac{1}{k} = \frac{1}{n}\sum_{i=1}^{n} \ln N_i^k \tag{17}$$

Solve the implicit function (17) by using MATLAB, and bring the value of k into Eq. 14 to solve for the value of t. According to the relationship between k, t, and λ, solve for the value of λ. The results are listed in Table.11. The Weibull cumulative probability and probability density curves for all experimental groups under different freeze-thaw cycles and stress levels are plotted in Figure 19. These plots illustrate the distribution of fatigue life for recycled aggregate concrete (RAC) under varying conditions.

A clear trend emerges from the Weibull plots: as the number of freeze-thaw cycles increases, the randomness and variability in the fatigue life of RAC also increase. This phenomenon can be explained by the heightened inhomogeneity in the concrete caused by freeze-thaw damage, which introduces randomly distributed pores and cracks. These defects compromise the material's structural integrity, leading to greater variability in fatigue performance.

However, there are some exceptions to this trend, particularly in cases such as the control group (C) at a stress level of 0.6, SI-M at a stress level of 0.6, and SS-M at a stress level of 0.8. These anomalies could be attributed to variations in the composition of the recycled aggregates (RAs) used in these specific mixtures. It is possible that the recycled aggregates contain varying proportions of natural aggregates, or the presence of residual old cement paste introduces different levels of initial defects, such as pores and microcracks. These compositional differences may lead to deviations from the expected fatigue life behavior, as observed in the exceptions mentioned.

The results indicate that, while freeze-thaw damage increases the variability of fatigue life in most cases, the composition and quality of recycled aggregates play a significant role in determining the overall fatigue performance of RAC. These findings underscore the importance of understanding the properties of recycled aggregates and their influence on the long-term durability of concrete under cyclic loading and environmental stress.

Table.11 Results of parameter estimation

Group	Stress level	Freeze-thaw 0 cycles		Freeze-thaw 70 cycles		Freeze-thaw 140 cycles	
		k	lamb	k	lamb	k	lamb
C	0.8	5.31	5296.00	3.57	2496.40	3.24	848.51
	0.7	4.76	21597.00	3.06	11368.00	3.40	4710.50
	0.6	3.82	56773.00	3.69	30458.00	3.92	18245.00
SI-M	0.8	5.48	3788.00	3.82	2067.50	3.01	1406.80
	0.7	4.55	16965.00	4.46	10038.00	4.02	5178.20
	0.6	4.31	41676.00	3.86	27420.00	4.50	20842.00
S-M	0.8	4.98	84190.00	4.29	55055.00	3.59	38214.00
	0.7	4.80	345340.00	4.24	233530.00	3.89	178530.00
	0.6	3.60	946060.00	3.58	671480.00	3.55	541310.00
SS-M	0.8	5.55	171540.00	5.72	114610.00	5.05	86385.00
	0.7	4.67	716930.00	3.89	505680.00	3.61	405260.00
	0.6	4.88	1795300.00	3.79	1341500.00	3.46	949040.00
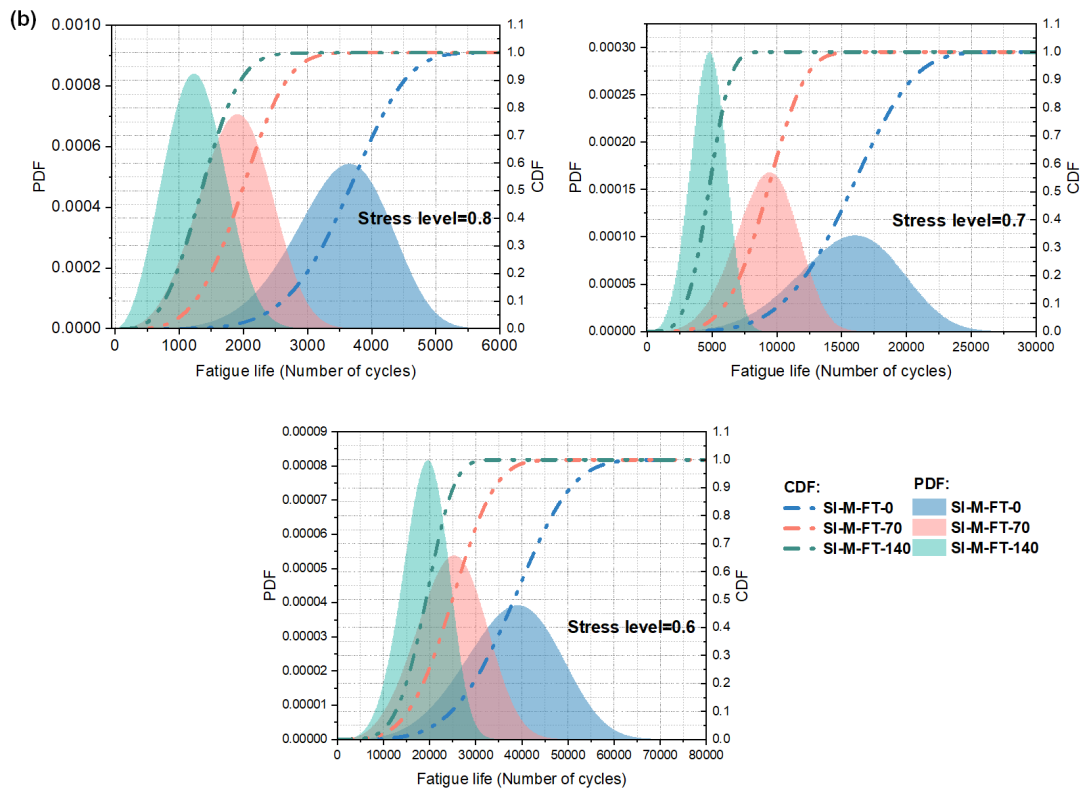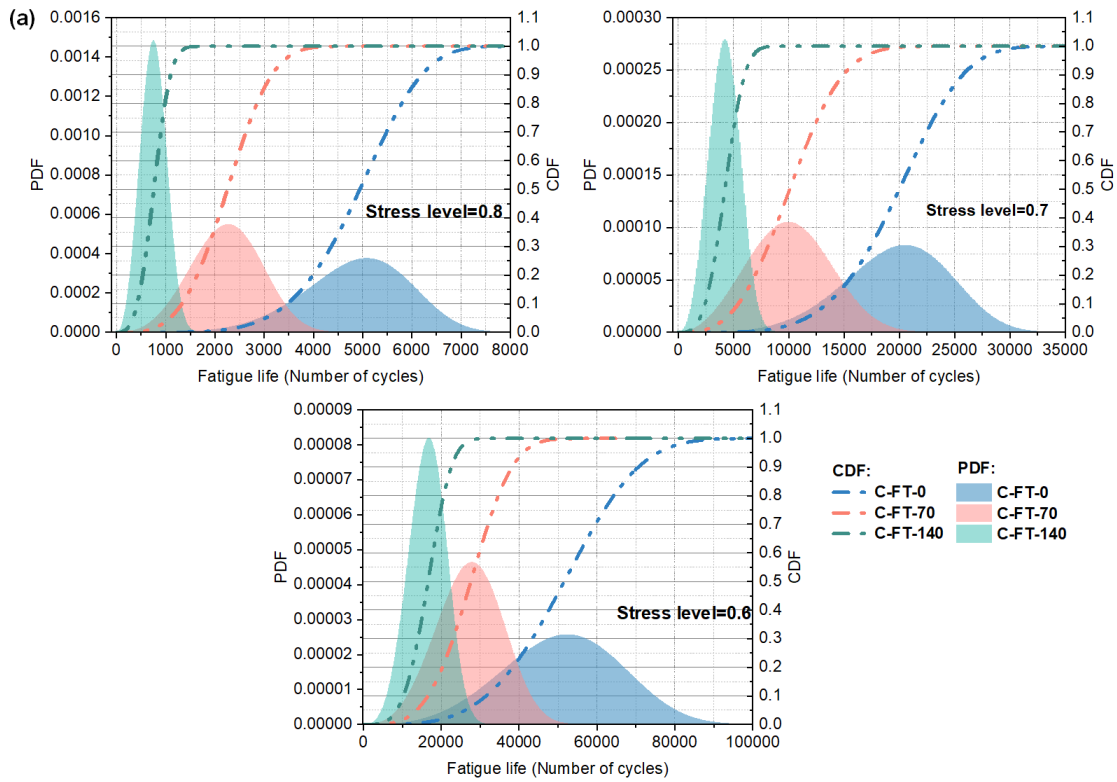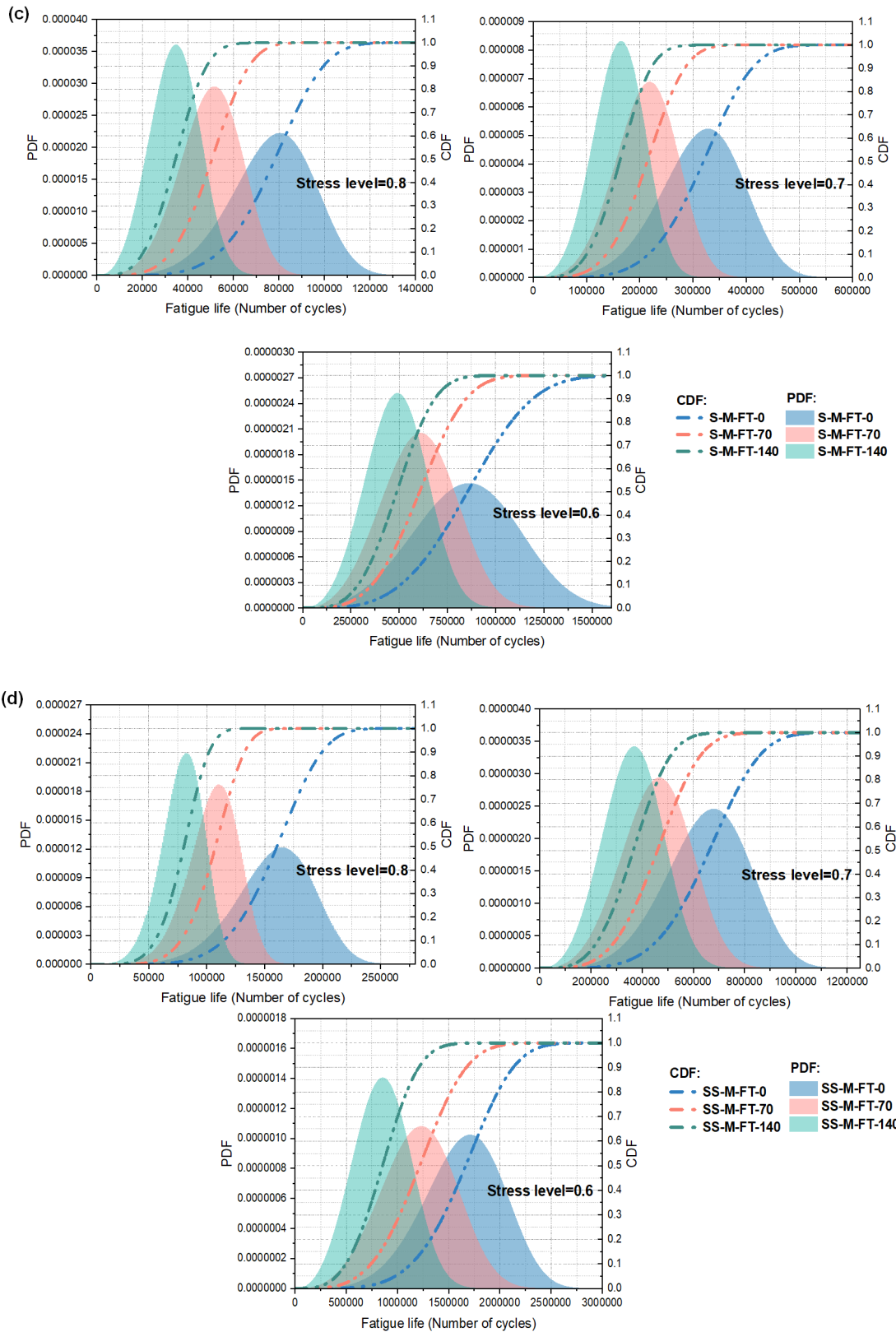
The prediction model of fatigue life

The fatigue life of recycled aggregate concrete (RAC) is significantly influenced by factors such as stress levels, freeze-thaw damage, and different modification techniques. In this section, fatigue life prediction models for RAC, incorporating these variables, have been developed, as shown in Eq. 18. The models account for the effects of the different modifications and the number of freeze-thaw cycles, providing a comprehensive framework for predicting the fatigue life of RAC under various conditions.

The high values of R^2 indicating the goodness of fit for the established models, demonstrate the reliability and accuracy of the predictive models. These strong correlation values suggest that the models effectively capture the relationship between fatigue life, stress levels, freeze-thaw damage, and the modification methods applied to RAC.

The established models, validated by the data, can be utilized in the fatigue design of RAC. Engineers and researchers can apply these models to predict the expected fatigue life of RAC in different structural applications, allowing for the optimization of materials and design strategies to enhance the durability and performance of concrete structures exposed to cyclic loading and environmental stressors.

$$
\begin{aligned}
&C : \log_{10}(N) = -0.00474 \bullet F - 5.72407 \bullet S + 8.22823 \quad (R^2 = 0.917) \\
&SI\text{-}M : \log_{10}(N) = -0.00308 \bullet F - 5.57664 \bullet S + 7.9889 \quad (R^2 = 0.927) \\
&S\text{-}M : \log_{10}(N) = -0.00213 \bullet F - 5.41581 \bullet S + 9.20543 \quad (R^2 = 0.912) \\
&SS\text{-}M : \log_{10}(N) = -0.00209 \bullet F - 5.14794 \bullet S + 9.33190 \quad (R^2 = 0.908)
\end{aligned}
\tag{18}
$$

Where N is the flexural fatigue life, S is the stress level, and F refers to the freeze-thaw cycle.
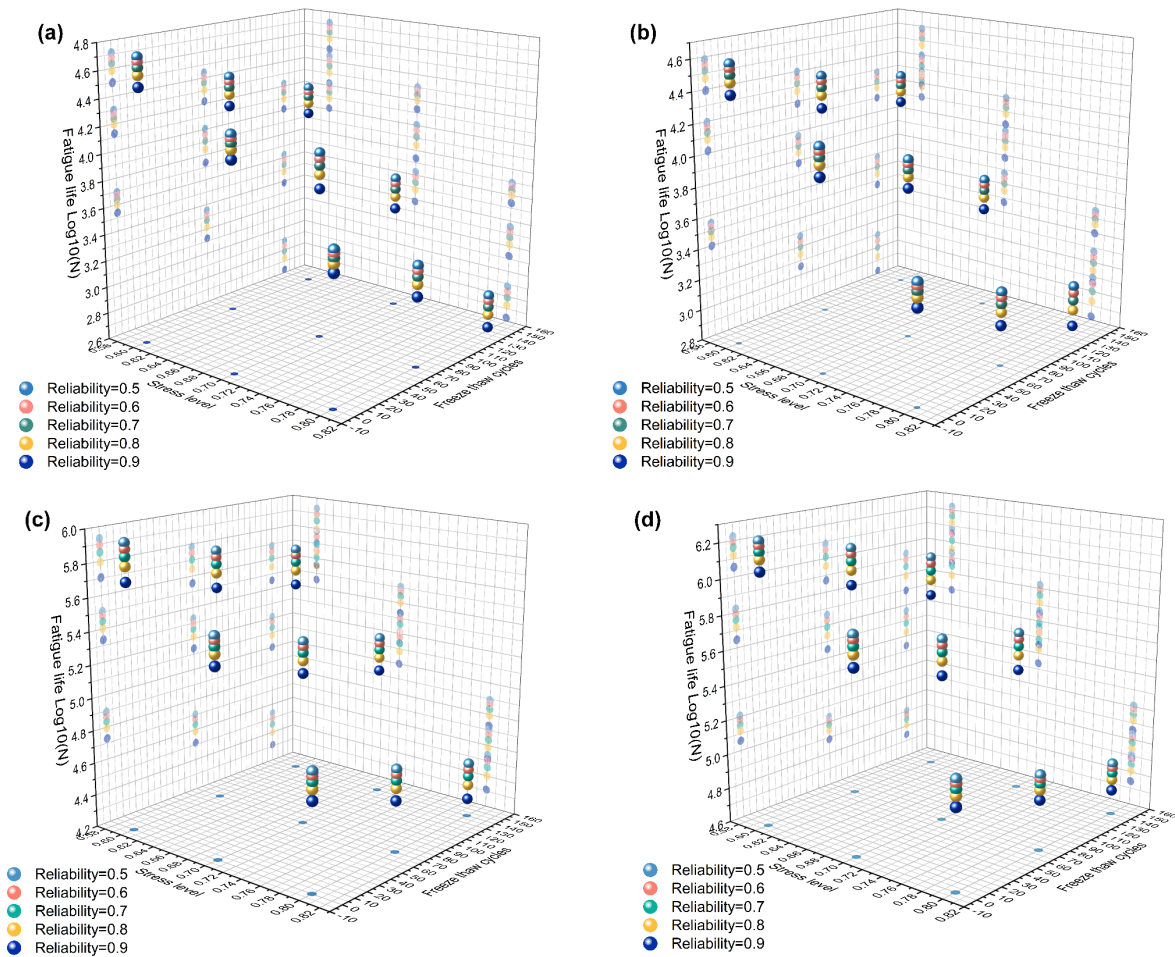
Fig.20 Predicted flexural fatigue life with varying reliability; (a) C; (b)SI-M; (c) S-M; (d) SS-M

The fatigue life of concrete materials is inherently variable and subject to significant randomness, making the geometric mean an unsuitable metric for accurately representing characteristic fatigue life. To address this issue, reliability theory offers a robust approach. The Weibull reliability function, as outlined in Equation 8, provides a means of calculating fatigue life at various reliability levels, which can then be used to establish fatigue life prediction models for different reliability thresholds.

In this context, the Weibull reliability function enables the estimation of fatigue life corresponding to reliability levels of 0.5, 0.6, 0.7, 0.8, and 0.9. These reliability levels represent the probability that a specimen will survive beyond a certain fatigue life, given specific stress levels and environmental conditions, such as freeze-thaw cycles. Figure 20 illustrates the predicted flexural fatigue life of RAC samples subjected to different stress levels and freeze-thaw cycles based on these reliability thresholds.

The reliability-based fatigue life prediction models, which account for both stress levels and the number of freeze-thaw cycles, are critical for designing more durable RAC structures. By incorporating reliability theory, these models allow for more accurate predictions of fatigue performance under real-world conditions. The fatigue life models established for various reliability levels are provided below, offering a

practical tool for engineers and designers to estimate the expected lifespan of concrete structures under varying degrees of uncertainty and environmental stress.

These models provide a comprehensive framework for the fatigue design of RAC, allowing for the incorporation of reliability factors into design decisions to ensure the long-term performance and durability of concrete in infrastructure applications exposed to cyclic loading and harsh environmental conditions.

$$C : \begin{cases} Reliability = 0.5 : \log_{10}(N) = -5.745S - 0.00472F + 8.266 \quad (R^2 = 0.976) \\ Reliability = 0.6 : \log_{10}(N) = -5.743S - 0.00478F + 8.233 \quad (R^2 = 0.975) \\ Reliability = 0.7 : \log_{10}(N) = -5.740S - 0.00485F + 8.196 \quad (R^2 = 0.975) \\ Reliability = 0.8 : \log_{10}(N) = -5.737S - 0.00495F + 8.146 \quad (R^2 = 0.935) \\ Reliability = 0.9 : \log_{10}(N) = -5.731S - 0.00510F + 8.065 \quad (R^2 = 0.970) \end{cases} \quad (19)$$

$$SI-M : \begin{cases} Reliability = 0.5 : \log_{10}(N) = -5.574S - 0.00303F + 8.005 \quad (R^2 = 0.982) \\ Reliability = 0.6 : \log_{10}(N) = -5.589S - 0.00309F + 7.987 \quad (R^2 = 0.980) \\ Reliability = 0.7 : \log_{10}(N) = -5.605S - 0.00315F + 7.965 \quad (R^2 = 0.979) \\ Reliability = 0.8 : \log_{10}(N) = -5.627S - 0.00323F + 7.936 \quad (R^2 = 0.977) \\ Reliability = 0.9 : \log_{10}(N) = -5.661S - 0.00336F + 7.890 \quad (R^2 = 0.972) \end{cases} \quad (20)$$

$$S-M : \begin{cases} Reliability = 0.5 : \log_{10}(N) = -5.447S - 0.00213F + 9.247 \quad (R^2 = 0.985) \\ Reliability = 0.6 : \log_{10}(N) = -5.419S - 0.00217F + 9.199 \quad (R^2 = 0.984) \\ Reliability = 0.7 : \log_{10}(N) = -5.386S - 0.00222F + 9.140 \quad (R^2 = 0.982) \\ Reliability = 0.8 : \log_{10}(N) = -5.343S - 0.00228F + 9.063 \quad (R^2 = 0.979) \\ Reliability = 0.9 : \log_{10}(N) = -5.274S - 0.00238F + 8.941 \quad (R^2 = 0.976) \end{cases} \quad (21)$$

$$SS-M : \begin{cases} Reliability = 0.5 : \log_{10}(N) = -5.161S - 0.00202F + 9.357 \quad (R^2 = 0.977) \\ Reliability = 0.6 : \log_{10}(N) = -5.115S - 0.00207F + 9.298 \quad (R^2 = 0.978) \\ Reliability = 0.7 : \log_{10}(N) = -5.062S - 0.00213F + 9.230 \quad (R^2 = 0.979) \\ Reliability = 0.8 : \log_{10}(N) = -4.992S - 0.00221F + 9.140 \quad (R^2 = 0.981) \\ Reliability = 0.9 : \log_{10}(N) = -4.881S - 0.00234F + 8.997 \quad (R^2 = 0.983) \end{cases} \quad (22)$$

Findings on numerical simulation on recycled aggregate concrete slab

The numerical analysis conducted in this study aimed to develop a recycled aggregate concrete (RAC) pavement slab section and assess its maximum load-carrying capacity. To achieve this, ATENA Studio version 5.9.2c—a non-linear analysis tool developed by Cervenka Consulting—was employed. This software is capable of simulating the actual degradation behavior of concrete, including steel rebar yielding and concrete crushing within concrete structures. For the purpose of this analysis, the CC3DNonLinCementitious2 model was utilized to incorporate fracture-plastic constitutive relations that account for the non-linear behavior of concrete, as shown in Figure 21.

The material properties used in the numerical model included key parameters such as compressive strength, tensile strength, Poisson's ratio, and modulus of elasticity of the concrete. Before conducting the full-scale analysis of the RAC pavement slab, a validation step was performed by modeling cylindrical concrete specimens using the GiD program, which is used for the geometric modeling and data input required for numerical simulation. This validation in ATENA was necessary to ensure that the numerical model would behave as closely as possible to the actual specimens tested in the laboratory for compressive strength.

In this validation phase, a concrete cylinder with a diameter of 100 mm and a height of 200 mm—identical to the laboratory-tested specimens—was modeled, as shown in Figure 22. The bottom surface of the cylinder was fully supported, restricting all translational movements, while a prescribed displacement of 3 mm was applied to the top surface in 20 load increments. Reaction forces at the bottom support and displacement in the z-direction at the top surface were monitored throughout the loading process to capture the mechanical behavior of the concrete cylinder.

This validation process aimed to develop a reliable numerical model that accurately replicates the experimental compressive strength test results. Once the numerical model was validated, it was used to conduct further analysis on the RAC pavement slab section, focusing on its load-carrying capacity under different loading conditions. By using ATENA's advanced capabilities to simulate concrete degradation, yielding of steel reinforcement, and concrete crushing, the study provides critical insights into the behavior of RAC in structural applications, offering a reliable method for analyzing RAC pavement slabs under real-world load scenarios.
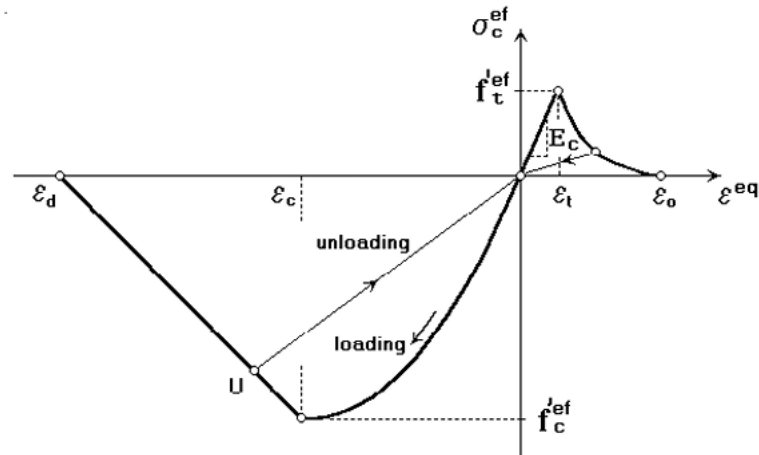
CIAMTIS
U.S. DOT Region 3 University Transportation Center

Fig. 21 Constitutive stress-strain relation for CC3DNonLinCementitious2 model in ATENA
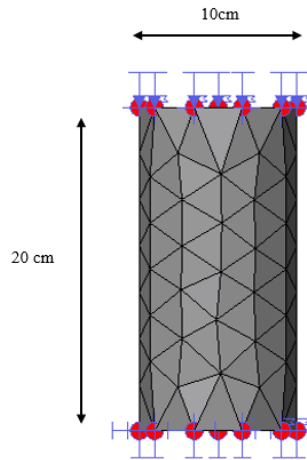

Fig. 22 Geometry and boundary condition of concrete cylinder

The geometry of the pavement slab model was designed with dimensions of 3040 mm in width, 10360 mm in length, and 230 mm in thickness, as illustrated in Figure 23. For the loading surfaces, an Elastic 3D material was selected using the CC3DElastIsotropic material prototype [40], which is appropriate for simulating the elastic behavior of the concrete under load. For the reinforcement, 1D Reinforcement elements were chosen to represent the steel bars, with a characteristic yield strength of 500 MPa to replicate the behavior of the steel reinforcement in the slab.

To simulate realistic loading conditions, rigid plates were introduced at locations on the slab corresponding to where the wheels of an HL-93 truck would generate maximum loading. The loading was applied by prescribing a uniform vertical displacement of approximately 5 mm on the top surface of the steel plates. This displacement mimics the loading that would occur in real-world conditions. Monitors were placed at the center of the top loading surfaces of the slab to record both the displacement and the maximum load in the z-direction, enabling the generation of a load-displacement diagram. This diagram is crucial for understanding the mechanical behavior of the slab under loading.

The boundary conditions for the slab were applied to the side surfaces as x-y constraints, based on field observations of how slabs are typically constrained in pavement structures. Since the loading surfaces (rigid plates) and the slab's top surface are independent, a fixed contact condition was introduced between these surfaces to prevent any sliding during the analysis. The top loading surfaces were designated as slave surfaces, while the slab's top surface was treated as the master surface in the contact pair. This master-slave surface relationship is important in finite element analysis to ensure proper interaction between the two surfaces during load application.

In finite element analysis, the quality of the mesh plays a critical role in determining the accuracy of the results, as well as the computational efficiency in terms of memory usage and processing speed. For this reason, a structured meshing method was employed, using hexahedral elements with a mesh size of 0.1. Hexahedral elements provide better accuracy in simulating the behavior of solid structures compared to other element types, and the chosen mesh size strikes a balance between computational efficiency and the accuracy of the analysis results.

This model setup, including the geometric configuration, material properties, boundary conditions, and meshing, allowed for a detailed analysis of the slab's load-carrying capacity under realistic loading conditions. The combination of well-defined material models, boundary conditions, and structured meshing ensures that the finite element analysis results are reliable and can be used to evaluate the performance of RAC pavement slabs in field conditions.
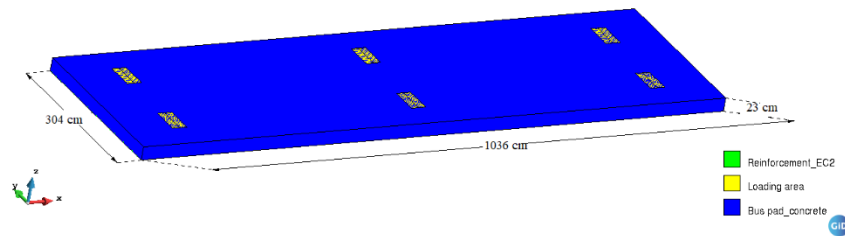
Fig. 23 Geometry of pavement section model

For concrete pavement sections, the load-carrying capacity is significantly influenced by the underlying subgrade soil, which acts as an elastic foundation. As mentioned in previous studies [51], the interaction between the pavement and subgrade plays a crucial role in determining the structural performance of the pavement. To account for this, the concrete pavement section model was further analyzed by incorporating various subgrade reaction moduli to assess the impact of subgrade stiffness on the maximum load-carrying capacity. The subgrade soil in the model was represented as a Winkler foundation, which idealizes the subgrade as a system of evenly spaced, independent linear springs. These springs act upward on the bottom face of the pavement section, simulating the support provided by the subgrade [41-44]. The stiffness of each spring corresponds to the subgrade modulus (also known as the modulus of subgrade reaction), which represents the spring constant for the soil layer supporting the pavement. This subgrade modulus quantifies the relationship between the soil's reaction force and the deflection of the pavement above it.

The Winkler foundation model is widely used in pavement design because it simplifies the complex interaction between the pavement and the subgrade into a system of discrete, independent springs. Each spring provides a reactive force proportional to the vertical displacement of the pavement section, and the overall stiffness of the foundation is directly influenced by the subgrade modulus. In the analysis, different values of subgrade reaction modulus were applied to evaluate how variations in the stiffness of the underlying soil affect the load-carrying capacity of the pavement. This approach allows for a more accurate assessment of the pavement's performance in real-world conditions, where the supporting soil may vary in stiffness due to factors such as moisture content, compaction, and soil type. By analyzing the model with varying subgrade moduli, the study provides insights into how different soil conditions influence the structural behavior of RAC pavement sections, enabling engineers to optimize pavement designs based on the characteristics of the subgrade. This is particularly important for ensuring the durability and longevity of pavement structures, as the interaction

between the pavement and subgrade is a key determinant of performance under loading conditions.

In this section, three batches of concrete mixes were developed, differentiated by water-cement (w/c) ratios of 0.35, 0.45, and 0.55. Recycled coarse aggregate (RCA) was incorporated in varying percentages, specifically 50%, 70%, and 100%. Each batch also included a reference mix with no RCA, allowing for comparison with two types of modified RCA mixes: water-soaked RCA and silane surface-treated RCA.

The coarse aggregates were used in saturated surface dry (SSD) conditions, and the water-cement ratio for each mix was adjusted based on the water absorption and moisture content of the coarse aggregate. This adjustment ensured the consistency of the mix design and avoided excess water in the mix, which could otherwise alter the intended properties of the concrete.

Concrete mixes were designated based on the treatment method, water-cement ratio, and percentage of RCA used. For example:

CRM-35-50 indicates a control mix with a 0.35 w/c ratio and 50% RCA.

WRM designates a mix with water-soaked RCA.

SRM refers to a mix with silane surface-modified RCA.

SIM indicates a mix where silane was integrated into the cement matrix.

The detailed proportions of these mixes are provided in Table 12.

For the evaluation of freeze-thaw durability, the concrete batch with a 0.35 w/c ratio was selected. In addition to the standard surface modification methods, a new technique, the silane integrated method (SIM), was introduced. In this method, a silane emulsion solution was directly added to the concrete during the mixing process, allowing for a more integrated modification of the cement matrix. This approach was aimed at enhancing the freeze-thaw resistance of the concrete by reducing water absorption and improving the overall durability of the RAC.

The inclusion of different treatment methods, RCA percentages, and water-cement ratios allows for a comprehensive analysis of how these variables affect the durability, mechanical performance, and freeze-thaw resistance of RAC. The findings from this study are critical for optimizing the use of recycled aggregates in concrete, particularly in environments where freeze-thaw cycles are a significant concern.

Table 12 Mix proportioning

Batch	Control Mix	Water-soaked Mix	Silane surface modified Mix	Silane integrated Mix	w/c ratio	RCA replacement ratio (wt. %)	Cement	Fine aggregate	Natural coarse aggregate	Recycled coarse aggregate

Group				w/c	RCA %	kg/m³			
B1	CRM-35-0				0.35	0	929	923	1917	0
	CRM-35-50	WRM-35-50	SRM-35-50	-	0.35	50	929	923	959	959
	CRM-35-70	WRM-35-70	SRM-35-70	-	0.35	70	929	923	575	1342
	CRM-35-100	WRM-35-100	SRM-35-100	SIM-35-100	0.35	100	929	923	0	1917
B2	CRM-45-0				0.45	0	722	1096	1917	0
	CRM-45-50	WRM-45-50	SRM-45-50	-	0.45	50	722	1096	959	959
	CRM-45-70	WRM-45-70	SRM-45-70	-	0.45	70	722	1096	575	1342
	CRM-45-100	WRM-45-100	SRM-45-100	-	0.45	100	722	1096	0	1917
B3	CRM-55-0				0.55	0	591	1206	1917	0
	CRM-55-50	WRM-55-50	SRM-55-50	-	0.55	50	591	1206	959	959
	CRM-55-70	WRM-55-70	SRM-55-70	-	0.55	70	591	1206	575	1342
	CRM-55-100	WRM-55-100	SRM-55-100	-	0.55	100	591	1206	0	1917

Note: CRM stands for control RCA mix with no surface treatment, SRM stands for silane surface treated RCA mix and SIM stands for silane into cement base mix.

For validation purposes, concrete cylinder models were analyzed for their load-displacement behavior using ATENA Studio, and the results were compared with those obtained from laboratory experiments. The material properties used in the numerical model included compressive strength, tensile strength, Poisson's ratio, and modulus of elasticity. The failure patterns observed during the experimental testing of the cylinder crushing were found to be closely aligned with the failure patterns obtained from the numerical analysis in ATENA, as illustrated in Figure 24.

To further validate the model, the peak loads obtained from the numerical analysis for each batch of different water-cement (w/c) ratios (0.35, 0.45, and 0.55) and various RCA replacement ratios (50%, 70%, and 100%) were compared with the experimental results. As shown in Figure 25, the peak loads from the numerical analysis closely matched those from the experimental tests. The ratio between the experimental and numerical results for all concrete mixes ranged from 0.97 to 1.05, demonstrating a high level of agreement between the two methods.

This close correlation between the experimental and numerical results validates the accuracy of the numerical model developed in ATENA Studio. With this validation, the model can be confidently used for further analysis of the RAC pavement section, ensuring that it reliably

represents the structural behavior of the material under loading conditions. This validation step is crucial for confirming the model's ability to simulate real-world scenarios accurately and for applying it to more complex structural analyses in the study.
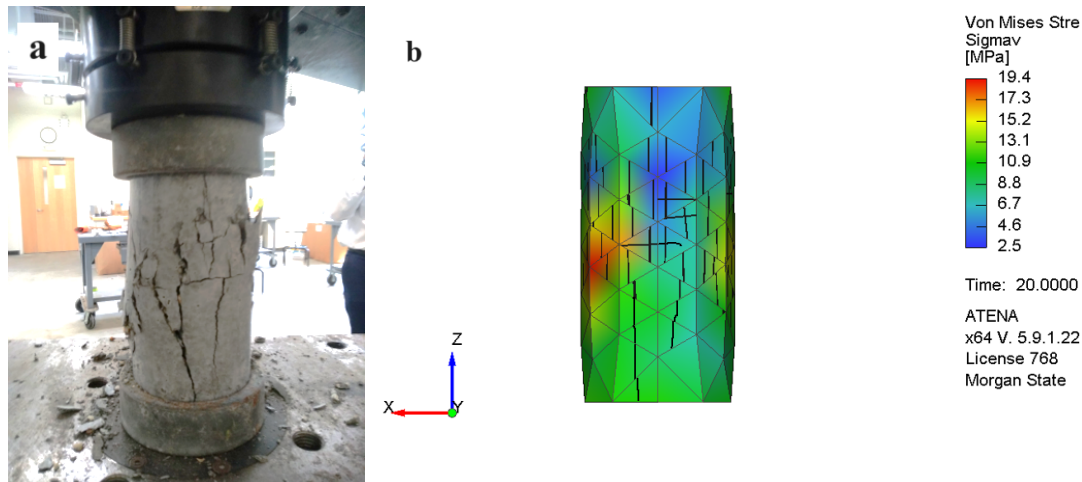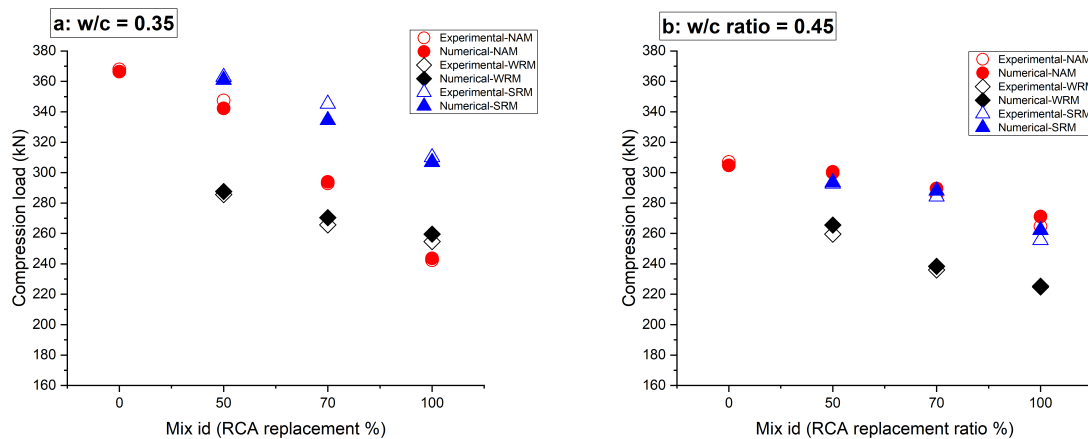

Fig. 24 Failure pattern of concrete cylinder during (a) Experimental testing, and (b) Numerical analysis
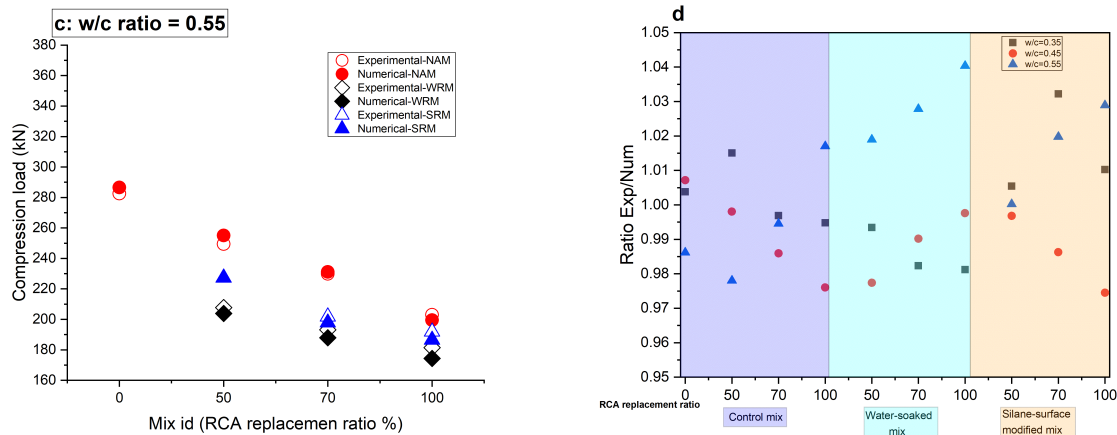
Fig. 25 Comparison of peak compression loads for various concrete mixes having w/c ratio of (a) 0.35 (b) 0.45, and (c) 0.55 (d) Ratio of experimental to numerical compression loads versus concrete mixes.

A further analysis was conducted on a concrete pavement slab model based on the experimental properties of silane-modified recycled aggregate concrete (SRM), focusing on the load-carrying capacity. In addition to the control mixes (without RCA), the concrete mixes SRM-35-50, SRM-45-50, and SRM-55-50, which included silane surface-treated recycled aggregates with a 50% RCA content, were selected for the numerical analysis. These mixes demonstrated superior mechanical and freeze-thaw durability properties compared to other mixes in this study, making them suitable candidates for further investigation.

The numerical analysis of the RAC pavement slab sections was carried out using ATENA Studio, and the resulting load-displacement curves are presented in Figure 26. The results revealed that pavement sections based on the CRM-35-0 (control mix) and SRM-35-50 (silane-modified, 50% RCA) mixes exhibited similar peak load-carrying capacities, with only a 0.61% difference between them. This close agreement suggests that the silane surface modification technique effectively maintains the load-bearing capacity of RAC at a low w/c ratio (0.35), comparable to that of conventional concrete without RCA.

However, as the w/c ratio increased, the peak load-carrying capacity of the pavement sections declined. The variability between the peak loads of the control mix and the silane surface-

modified mix increased, with differences of 2.61% and 10.75% at w/c ratios of 0.45 and 0.55, respectively. This indicates that higher w/c ratios reduce the mechanical performance of both the control and modified concrete, although the silane-modified mixes still performed reasonably well compared to the control.

The study also examined the influence of subgrade soil stiffness on the load-carrying capacity of the pavement sections. It was found that stiffer soil beneath the pavement resulted in a more uniform distribution of the load over the slab, while more flexible soil caused the load to be distributed locally, leading to reduced performance. The analysis was performed for various stiffness values of the underlying soil, and it was observed that increasing the soil stiffness significantly improved the load-carrying capacity of the pavement sections.

Specifically, when the soil stiffness increased from 20 to 40, 60, 80, and 100 kN/m²/m, the peak load-carrying capacity of the pavement sections increased by 6.15%, 20.65%, 32.92%, and 47.60%, respectively. These results emphasize the importance of soil stiffness in the structural performance of pavement systems, as stiffer subgrade soils enhance the load distribution and increase the overall load-bearing capacity of the pavement.

In conclusion, the numerical analysis validated that silane surface modification can enhance the performance of RAC, particularly at lower w/c ratios. However, the load-carrying capacity declines as the w/c ratio increases. Additionally, the stiffness of the supporting soil plays a crucial role in determining the maximum load-carrying capacity of the pavement, with higher stiffness values leading to significantly better performance. These insights provide valuable information for optimizing RAC pavement designs, particularly in regions subject to freeze-thaw cycles and varying soil conditions.

Von Mises Stre
Sigmav
[MPa]

9.5
8.3
7.1
5.9
4.7
3.6
2.4
1.2
0.0

Deformation sc
1075.0143

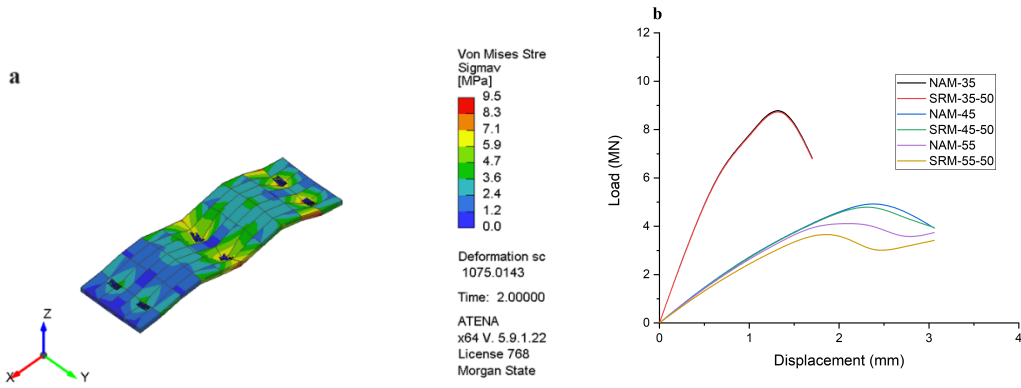Time: 2.00000

ATENA
x64 V. 5.9.1.22
License 768
Morgan State

Fig. 26 (a) Analysis of pavement section in ATENA studio (b) Load-displacement curves of pavement sections

Recommendations and conclusions

Conclusions

This study comprehensively examined the durability and fatigue life of recycled aggregate concrete (RAC) prepared with various modification techniques. These techniques included surface modifications of recycled aggregates using silane emulsion (S-M) and sodium silicate (SS-M), as well as cement matrix modification using silane emulsion (SI-M). The performance of these modified RAC mixtures was evaluated through a range of tests, including measurements of water permeability, compressive strength, flexural strength, mass loss, and relative dynamic elastic modulus, particularly under conditions of freeze-thaw cycling. Additionally, the microstructure of the modified recycled aggregates and the interfacial transition zone (ITZ) between the recycled aggregates and the new cement matrix were investigated using scanning electron microscopy (SEM) and backscattered electron (BSE) imaging. These techniques helped to elucidate the mechanisms underlying the effects of different modification methods. The flexural fatigue life of RAC under varying freeze-thaw cycles and stress levels was also investigated, and the impact of these factors on fatigue life was analyzed in detail. The key findings of this study are summarized below:

Enhanced Mechanical Performance through Surface Modifications:

The application of silane and sodium silicate surface modifications significantly improved the mechanical performance and freeze-thaw resistance of RAC, which could potentially expand its use in cold climates where freeze-thaw damage is a major concern. The study showed that these surface modifications reduced the water permeability of RAC, resulting in enhanced durability. The improvement in strength and freeze-thaw resistance can be primarily attributed to the better properties of the recycled aggregates and the densification of the ITZ. In the case of silane surface modification, the formation of a hydrophobic silicon film on the surface of the recycled aggregates prevents excessive water accumulation. This hydrophobic layer reduces the local water content, leading to a denser ITZ. Additionally, the reduction in water absorption due to the hydrophobic film hinders water transmission through the RA, further enhancing freeze-thaw resistance. Sodium silicate surface modification filled the initial pores and cracks of the RA, and the chemical reaction between silicate ions and calcium hydroxide formed calcium silicate hydrate (C-S-H) gel on the surface of the recycled aggregates. These reactions significantly

reduced the water absorption capacity of RA and promoted greater hydration in the ITZ, leading to enhanced mechanical performance and freeze-thaw durability.

Cement Matrix Modification and Its Effects:

The incorporation of silane emulsion in the cement matrix improved the freeze-thaw resistance of RAC by enhancing the water diffusion resistance of the concrete. However, the BSE analysis revealed that this improvement came at a cost to the cement hydration process. The introduction of silane emulsion led to the formation of a hydrophobic silicon membrane within the capillary pores of the cement matrix, which restricted water access to the cement particles and, consequently, reduced cement hydration. As a result, the porosity of the cement matrix increased, leading to a reduction in compressive strength. Despite the enhanced freeze-thaw durability, the strength loss due to increased porosity highlights the trade-offs associated with using silane emulsion in the cement matrix. While the improved resistance to water diffusion and freeze-thaw cycles is beneficial, the reduction in hydration must be carefully considered in structural applications.

Crack Formation in ITZ and Recycled Aggregates:

The study highlighted that the ITZ and RA, in addition to the new cement matrix, are critical regions affected by freeze-thaw damage. The formation of cracks within the cement matrix, particularly around macropores due to water diffusion and the freeze-thaw process, can extend to the ITZ and recycled aggregates. These cracks compromise the structural integrity of RAC, underscoring the importance of improving the surface properties of recycled aggregates and strengthening the ITZ. By enhancing the properties of these regions, the overall freeze-thaw durability of RAC can be significantly improved. The study emphasizes that effective surface modifications of recycled aggregates and ITZ improvements are key strategies for mitigating the propagation of cracks and enhancing the long-term durability of RAC in harsh environmental conditions.

Impact of Stress Levels and Modifications on Fatigue Life:

The flexural fatigue life of RAC was shown to decrease with increasing stress levels. Additionally, freeze-thaw damage resulted in a significant reduction in fatigue life, as expected. The analysis revealed that, among the factors considered, stress levels and the different modification techniques had a more pronounced effect on flexural fatigue life than freeze-thaw cycles alone. RAC prepared with silane surface modification (S-M) and sodium silicate surface modification (SS-M) exhibited better fatigue performance during freeze-thaw damage compared to both the control group (C) and the silane-modified cement matrix group (SI-M). Surface modifications of the aggregates also reduced the sensitivity of fatigue life to stress levels, which

is attributed to the improvements in the ITZ and the physical properties of the recycled aggregates. The SI-M group exhibited less flexural fatigue life loss under freeze-thaw damage due to improved freeze-thaw resistance, but the initial fatigue life was reduced due to decreased cement hydration, a consequence of silane emulsion in the cement matrix.

Variability in Fatigue Life and Weibull Distribution:

The Weibull two-parameter model was used to describe the distribution of flexural fatigue life across the various RAC mixtures. The results indicated that the randomness and variability in fatigue life increased with the number of freeze-thaw cycles. This can be attributed to the increased inhomogeneity of RAC as freeze-thaw damage progresses, leading to the formation of randomly distributed pores and cracks. These defects compromise the uniformity of the material, making fatigue life more unpredictable as damage accumulates. The Weibull distribution provided an effective model for capturing this variability and allowed for a probabilistic assessment of fatigue life under different conditions.

Fatigue Life Prediction Models and Reliability:

Fatigue life prediction models for the control group (C), SI-M, S-M, and SS-M were developed by considering both stress levels and freeze-thaw cycles. In addition, reliability theory was applied to establish fatigue life prediction models for different reliability thresholds, including 0.5, 0.6, 0.7, 0.8, and 0.9. These models provide a valuable tool for the design and optimization of RAC in structural applications. By incorporating reliability thresholds, engineers can predict the expected fatigue life of RAC with varying degrees of confidence, allowing for more informed decision-making in the design of concrete structures subjected to cyclic loading and freeze-thaw conditions. The reliability-based models enhance the applicability of RAC in real-world conditions where durability and long-term performance are critical.

Numerical simulations on recycled aggregate concrete slab:

Numerical analysis of RAC pavement section proved that employing 50% silane surface modified RCA in concrete pavements resulted in the same load carrying capacity as by the concrete pavement without RCA. However, with the increase in the soil stiffness which can be obtained by proper compaction of the soil, the load carrying capacity can be further increased for the pavement. For example, the load carrying capacity was increased by 6.15, 20.65, 32.92 and 47.60% when the soil stiffness was increased from 20 to 40, 60, 80 and 100 $kN/m^2/m$, respectively.

.

References

[1] Hoornweg, D., & Pope, K. (2017). Population predictions for the world's largest cities in the 21st century. Environment and urbanization, 29(1), 195-216.

[2] Chen, Y., & Zhou, Y. (2020). The contents and release behavior of heavy metals in construction and demolition waste used in freeway construction. Environmental Science and Pollution Research, 27, 1078-1086.

[3] Datta, K., Chakraborty, S., & Roychoudhury, A. (2025). Management of soil, waste and water in the context of global climate change. In Environmental Nexus for Resource Management (pp. 1-26). CRC Press.

[4] Zhang, Z., Malik, M. Z., Khan, A., Ali, N., Malik, S., & Bilal, M. (2022). Environmental impacts of hazardous waste, and management strategies to reconcile circular economy and eco-sustainability. Science of The Total Environment, 807, 150856.

[5] Silva, R. V., De Brito, J., & Dhir, R. K. (2019). Use of recycled aggregates arising from construction and demolition waste in new construction applications. Journal of Cleaner Production, 236, 117629.

[6] Reis, G. S. D., Quattrone, M., Ambrós, W. M., Grigore Cazacliu, B., & Hoffmann Sampaio, C. (2021). Current applications of recycled aggregates from construction and demolition: A review. Materials, 14(7), 1700.

[7] Tam, V. W., Soomro, M., & Evangelista, A. C. J. (2018). A review of recycled aggregate in concrete applications (2000–2017). Construction and Building materials, 172, 272-292.

[8] Zhang, L. W., Sojobi, A. O., Kodur, V. K. R., & Liew, K. M. (2019). Effective utilization and recycling of mixed recycled aggregates for a greener environment. Journal of Cleaner Production, 236, 117600.

[9] Behera, M., Bhattacharyya, S. K., Minocha, A. K., Deoliya, R., & Maiti, S. (2014). Recycled aggregate from C&D waste & its use in concrete–A breakthrough towards sustainability in construction sector: A review. Construction and building materials, 68, 501-516.

[10] Silva, R. V., De Brito, J., & Dhir, R. K. (2017). Availability and processing of recycled aggregates within the construction and demolition supply chain: A review. Journal of Cleaner Production, 143, 598-614.

[11] Lu, C., Zhou, Q., Wang, W., Wei, S., & Wang, C. (2021). Freeze-thaw resistance of recycled aggregate concrete damaged by simulated acid rain. Journal of cleaner production, 280, 124396.

[12] Bao, J., Zheng, R., Yu, Z., Zhang, P., Song, Q., Xu, J., & Gao, S. (2022). Freeze-thaw resistance of recycled aggregate concrete incorporating ferronickel slag as fine aggregate. Construction and Building Materials, 356, 129178.

[13] Zhang, W., Liu, H., & Liu, C. (2022). Impact of rice husk ash on the mechanical characteristics and freeze–thaw resistance of recycled aggregate concrete. Applied Sciences, 12(23), 12238.

[14] Cheng, Y., Shang, X., & Zhang, Y. (2017, July). Experimental research on durability of recycled aggregate concrete under freeze-thaw cycles. In Journal of Physics: Conference Series (Vol. 870, No. 1, p. 012018). IOP Publishing.

[15] Richardson, A., Coventry, K., & Bacon, J. (2011). Freeze/thaw durability of concrete with recycled demolition aggregate compared to virgin aggregate concrete. Journal of Cleaner Production, 19(2-3), 272-277.

[16] Bogas, J. A., De Brito, J., & Ramos, D. (2016). Freeze–thaw resistance of concrete produced with fine recycled concrete aggregates. Journal of Cleaner Production, 115, 294-306.

[17] Wang, Y., Xie, M., & Zhang, J. (2023). Mechanical properties and damage model of modified recycled concrete under freeze-thaw cycles. Journal of Building Engineering, 78, 107680.

[18] Yu, Z., Zhang, H., Bao, J., Zhang, P., Ding, Y., Chen, X., ... & Song, Q. (2024). Coupled effects of the freeze-thaw cycles and salt erosion on the performance of recycled aggregate concrete. Journal of Building Engineering, 95, 110212.

[19] Júnior, N. A., Silva, G. A. O., & Ribeiro, D. V. (2018). Effects of the incorporation of recycled aggregate in the durability of the concrete submitted to freeze-thaw cycles. Construction and Building Materials, 161, 723-730.

[20] Hao, L., Liu, Y., & Xiao, J. (2021). Durability of recycled aggregate thermal insulation concrete under combined flexural loading and freeze–thaw cycles. Construction and Building Materials, 272, 121652.

[21] Kazmi, S. M. S., Munir, M. J., Wu, Y. F., Patnaikuni, I., Zhou, Y., & Xing, F. (2020). Effect of different aggregate treatment techniques on the freeze-thaw and sulfate resistance of recycled aggregate concrete. Cold Regions Science and Technology, 178, 103126.

[22] Wu, Q., Gong, F., Zhi, D., & Zhao, Y. (2022). Removing attached mortar from recycled aggregate by the combined freeze– thaw cycles and high‐ temperature drying. Structural Concrete, 23(5), 3126-3139.

[23] Xia, P., Yang, L., Wang, S., Gong, F., Cao, W., & Zhao, Y. (2023). Improved freeze-thaw modification of recycled concrete aggregate originally from frost resistive concrete. Cement and Concrete Composites, 144, 105302.

[24] Li, W., Cai, L., Wu, Y., Liu, Q., Yu, H., & Zhang, C. (2018). Assessing recycled pavement concrete mechanical properties under joint action of freezing and fatigue via RSM. Construction and Building Materials, 164, 1-11.

[25] Xue, G., Zhu, H., Xu, S., & Dong, W. (2023). Fatigue performance and fatigue equation of crumb rubber concrete under freeze–thaw cycles. International Journal of Fatigue, 168, 107456.

[26] Hao, L., Liu, Y., & Xiao, J. (2021). Durability of recycled aggregate thermal insulation concrete under combined flexural loading and freeze–thaw cycles. Construction and Building Materials, 272, 121652.

[27] Lei, B., Yu, L., Chen, T., Lv, Z., Zaland, S., & Tang, Z. (2023). Experimental study on the initial damage and mechanical property evolution of recycled coarse aggregates under freeze–thaw cycles and repeated loads. Construction and Building Materials, 375, 130972.

[28] ASTM C127-15, Standard Test Method for Density, Relative Density (Specific Gravity), and Absorption of Coarse Aggregate, ASTM International, West Conshohocken, PA, 2015, www.astm.org.

[29] Master Builders Solutions. MasterGlenium 7620 - High-Range Water-Reducing Admixture. Master Builders Solutions, www.master-builders-solutions.com.

[30] ASTM C131/C131M-20, Standard Test Method for Resistance to Degradation of Small-Size Coarse Aggregate by Abrasion and Impact in the Los Angeles Machine, ASTM International, West Conshohocken, PA, 2020, www.astm.org.

[31] ASTM C535-16, Standard Test Method for Resistance to Degradation of Large-Size Coarse Aggregate by Abrasion and Impact in the Los Angeles Machine, ASTM International, West Conshohocken, PA, 2016, www.astm.org.

[32] ASTM C39/C39M-23, Standard Test Method for Compressive Strength of Cylindrical Concrete Specimens, ASTM International, West Conshohocken, PA, 2023, www.astm.org.

[33] ASTM C78/C78M-22, Standard Test Method for Flexural Strength of Concrete (Using Simple Beam with Third-Point Loading), ASTM International, West Conshohocken, PA, 2022, www.astm.org.

[34] ASTM C1585-20, Standard Test Method for Measurement of Rate of Absorption of Water by Hydraulic-Cement Concretes, ASTM International, West Conshohocken, PA, 2020, www.astm.org.

[35] ASTM C666/C666M-15, Standard Test Method for Resistance of Concrete to Rapid Freezing and Thawing, ASTM International, West Conshohocken, PA, 2015, www.astm.org.

[36] ASTM C215-19, Standard Test Method for Fundamental Transverse, Longitudinal, and Torsional Frequencies of Concrete Specimens, ASTM International, West Conshohocken, PA, 2019, www.astm.org.

[37] Červenka, J., Červenka, V., & Laserna, S. (2018). On crack band model in finite element analysis of concrete fracture in engineering practice. Engineering Fracture Mechanics, 197, 27-47.

[38] Son, J., & Yang, S. (2022). A new approach to machine learning model development for prediction of concrete fatigue life under uniaxial compression. Applied Sciences, 12(19), 9766.

[39] Stalpers, L. J., & Kaplan, E. L. (2018). Edward L. Kaplan and the Kaplan-Meier survival curve. BSHM Bulletin: Journal of the British Society for the History of Mathematics, 33(2), 109-135.

[40] Ahmad, I., & Shokouhian, M. (2024). Promoting Sustainable Green Infrastructure: Experimental and Numerical Investigation of Concrete Reinforced with Recycled Steel Fibers. Archives of Advanced Engineering Science, 1-13.

[41] Das, A., Analysis of pavement structures. 2014: CRC Press.

[42] Mahrenholtz, O.H.J.A.o.A.M., Beam on viscoelastic foundation: an extension of Winkler's model. 2010. 80: p. 93-102.

[43] Kausel, E.J.S.D. and E. Engineering, Early history of soil–structure interaction. 2010. 30(9): p. 822-832.

[44]Ioannides, A.M.J.I.J.o.P.E., Concrete pavement analysis: the first eighty years. 2006. 7(4): p. 233-249.